Clustering Mechanism of Oxocarboxylic Acids Involving Hydration Reaction: Implications for the Atmospheric Models

Ling Liu,[1] Oona Kupiainen-Määttä,[2] Haijie Zhang,[1] Hao Li,[1] Jie Zhong,[3] Theo Kurtén,[4] Hanna Vehkamäki,[2] Shaowen Zhang,[1] Yunhong Zhang,[1] Maofa Ge,[5] Xiuhui Zhang,[1, a)] and Zesheng Li[1, b)]

[1)] *Key Laboratory of Cluster Science, Ministry of Education of China,*
School of Chemistry and Chemical Engineering, Beijing Institute of Technology,
Beijing 100081, China

[2)] *Institute for Atmospheric and Earth System Research/Physics,*
University of Helsinki, PO Box 64 (Gustaf Hällströmin katu 2a), FI-00014,
Helsinki, Finland

[3)] *Department of Chemistry, University of Nebraska-Lincoln, Lincoln, NE,*
USA 68588

[4)] *Institute for Atmospheric and Earth System Research/Chemistry,*
University of Helsinki, PO Box 64 (Gustaf Hällströmin katu 2a), FI-00014,
Helsinki, Finland

[5)] *Beijing National Laboratory for Molecular Sciences (BNLMS),*
State Key Laboratory for Structural Chemistry of Unstable and Stable Species,
Institute of Chemistry, Chinese Academy of Sciences, Beijing 100190,
China

(Dated: 4 May 2018)

The formation of atmospheric aerosol particles from condensable gases is a dominant source of particulate matter in the boundary layer, but the mechanism is still ambiguous. During the clustering process, precursors with different reactivities can induce various chemical reactions in addition to the formation of hydrogen bonds. However, the clustering mechanism involving chemical reactions is rarely considered in most of the nucleation process models. Oxocarboxylic acids are common compositions of secondary organic aerosol, but the role of oxocarboxylic acids in secondary organic aerosol formation is still not fully understood. In this paper, glyoxylic acid, the simplest and the most abundant atmospheric oxocarboxylic acids, has been selected as a representative example of oxocarboxylic acids in order to study the clustering mechanism involving hydration reaction using Density Functional Theory combined with the Atmospheric Clusters Dynamic Code. The hydration reaction of glyoxylic acid can occur either in the gas phase or during the clustering process. In atmospheric conditions, the total conversion ratio of glyoxylic acid to its hydration reaction product (2,2-dihydroxyacetic acid) in both gas phase and clusters can be up to 85%, and the product can further participate in the clustering process. The differences in cluster structures and properties induced by the hydration reaction lead to significant differences in cluster formation rates and pathways at relatively low temperatures.

---

[a] Electronic mail: zhangxiuhui@bit.edu.cn

[b] Electronic mail: zeshengli@bit.edu.cn

I. INTRODUCTION

Atmospheric aerosols have significant impacts on climate, weather and human health.[1,2] However, the formation mechanisms and composition of atmospheric aerosols are still not fully understood, and this constitutes one of the largest uncertainties in current atmospheric models.[3,4] There is compelling evidence that sulfuric acid (**SA**), water (**W**), ammonia (**A**) or amines can play key roles in atmospheric new particle formation (NPF), but these compounds are still not efficient enough to explain NPF in all the environments where it has been observed. Recently, numerous atmospheric observations and theoretical studies have shown that organic acids can also enhance NPF,[5–15] However, there are potentially tens of thousands of different atmospheric organic species with varying properties, which makes the exact chemical composition of clusters containing organic molecules highly speculative. Furthermore, different organics have different chemical reactivities. Thus, NPF may be driven not only by clustering processes, but also by various other complex and condition-dependent atmospheric chemical reactions.[16–23], which can influence the physical and chemical processes of NPF[24–26] . This makes the assessment of the role of organic compounds in the NPF process very complicated.

Oxocarboxylic acids are one of the most common organic species group found in secondary organic aerosol (SOA) in diverse environments. Experimental and theoretical studies have shown that the equilibrium reaction between carbonyl groups and the corresponding geminal diols can occur in the gas phase,[27–30] indicating that the gas-phase hydration reaction of oxocarboxylic acids may potentially occur along with the clustering process driving NPF. As the water concentration in the atmosphere is typically 8-10 orders of magnitude higher than that of other condensing species,[31] such hydration reactions are potentially of great

significance. However, in most present atmospheric aerosol formation models, the hydration

reactions of oxocarboxylic acids have been neglected due to the lack of information on them.

This may contribute to the discrepancy between measured and modeled results.[3,4] In this

study, we seek to understand the kinetics of atmospheric clustering processes involving hy-

dration reactions of oxocarboxylic acids under different atmospheric environments (different

precursor concentrations, relative humidities (RHs) and temperatures).

Experiments show that the gas-phase hydration reaction of glyoxylic acid (**GA**), the

simplest and the most abundant oxocarboxylic acids in the atmosphere,[32,33] is able to

form its geminal diol (**GW**).[27] Our previous theoretical study has also shown that this

process can be effectively catalyzed by different catalysts (**SA**, **W** or **A**), among which

SA is the most effective, lowering the activation free energy barrier from 38.56 to 9.48

kcal/mol.[34] Therefore, **GA** has been selected as a representative example of oxocarboxylic

acids in order to study the clustering mechanism involving hydration reaction. A combina-

tion of Density Functional Theory and the Atmospheric Clusters Dynamic Code (ACDC)[35]

has been used. As the hydrated clusters play an important role in cluster formation and

growth,[36] water (**W**)-containing clusters are included in our study. The studied system is

$(\mathbf{GA}/\mathbf{GW})_x \cdot (\mathbf{SA})_y \cdot \mathbf{A}_z \cdot \mathbf{W}_{0-n}$, where x is the number of **GA**/**GW** molecules in the clus-

ter, y is the number of **SA** molecules in the cluster, z is the number of **A** molecules in the

clusters, $x+y \geq z$ (i.e. only clusters that are acidic or chemically neutral are studied), and

$1 \leq x+y+z \leq 3$ (i.e. the studied clusters contain at most three molecules other than water).

The maximum number of water molecules in the cluster, n, depends on the cluster type,

and has been chosen so that all hydrates with relative abundance higher than 5% have been

included. There is always maximally one **GA** or **GW** molecule in the cluster.

II. COMPUTAIONAL METHODS

A. Quantum chemical calculations

The initial guesses for all the structures of clusters were generated by the ABCluster[37,38] program, which searches for global and local minima of molecular clusters using the artificial bee colony (ABC) algorithm. In ABCluster, water molecules were described by the TIP4P model and other molecules were described by the CHARMM36 force field.[39] First, about 1000 structures (for each cluster stoichiometry) were generated with ABCluster, and then these structures were optimized using the PM7 semiempirical method[40,41] using MOPAC2016[42]. Second, up to 100 structures with relatively low energies were selected for subsequently optimization with the M06-2X[43,44] density functional and a 6-31+G* basis set. Third, the 10 best of the resulting structures were further re-optimized by the M06-2X density functional with a 6-311++G(3df,3pd) basis set[45]. The M06-2X functional is one of the most successful functionals in describing noncovalent interactions,[43] and it has been successfully used to model the thermochemistry and equilibrium structures of atmospheric clusters.[46,47] The 6-311++G(3df,3pd) basis set was chosen based on its common use for atmospherically relevant clusters[48–51] and its excellent performance to estimate cluster properties when used in conjunction with the M06-2X functional.[46] We checked that the stable structures had positive vibrational frequencies. All the quantum chemistry calculations were performed using the Gaussian 09 program package.[52]

In additon, topological analysis was performed using atoms in molecules (AIM) theory with the Multiwfn package[53] to study the nature of hydrogen bonds. The wavefunctions (technically, electron densities) computed at the M06-2X/6-311++G(3df,3pd) level of theory were used to calculate the electron density ρ and Laplacian $\bigtriangledown^2 \rho$ at the bond critical points

5

[70] (BCPs).

B. Atmospheric Cluster Dynamics Code (ACDC) kinetic model

[72] The hydration reaction and clustering process of glyoxylic acids may coexist and compete

[73] against each other in the real atmosphere environment. Thus, it is necessary for cluster

[74] kinetic models to take into account the relevant chemical reactions to fully simulate the real

[75] NPF process in the atmosphere. The structural, thermodynamic and kinetic data generated

[76] by quantum chemistry calculations were used as input in cluster formation simulations

[77] performed using the Atmospheric Cluster Dynamics Code (ACDC)[35,54].

[78] The time development of the concentrations of each cluster was solved by integrat-

[79] ing numerically the birth-death equations[35] using the ode15s solver in MATLAB-R2013a

[80] program[55]. The birth-death equations can be written as

$$
\frac{dc_i}{dt} = \frac{1}{2}\sum_{j<i}\beta_{j,(i-j)}c_jc_{(i-j)} + \sum_j \gamma_{(i+j)\to i}c_{i+j} - \sum_j \beta_{i,j}c_ic_j
$$

$$
- \frac{1}{2}\sum_{j<i}\gamma_{i\to j}c_i + \sum_j k_{j\to i}c_j - \sum_j k_{i\to j}c_i + Q_i - S_i, \tag{1}
$$

[83] where c_i is the concentration of cluster i, $\beta_{i,j}$ is the collision coefficient between clusters i

[84] and j, $\gamma_{i\to j}$ is the evaporation coefficient of a molecule or a smaller cluster j from cluster

[85] i, Q_i is an outside source term of cluster i, and S_i is other possible sink term of cluster

[86] i. The coagulation sink coefficient corresponding to coagulation onto pre-existing larger

[87] particles was varied in the range of 10^{-3} s^{-1} to 5×10^{-3} s^{-1}, and the results indicate that our

[88] conclusions were not influenced by these variations.[56,57] Thus, a coagulation sink coefficient

[89] of 2.6×10^{-3} s^{-1} was used for all clusters.[56] $k_{i\to j}$ is the reaction rate coefficient of chemical

[90] reaction from reactant cluster i to product cluster j. The hydration reaction in **GA**-based

6

clusters can be uncatalyzed, or catalyzed by **SA**, **W** or **A**, as described in our previous study.[34] The nature of hydration reaction occurring in a certain **GA**-based cluster depends on the molecules the cluster contains, and the reaction rate corresponding to the catalyst molecule with the lowest activation free energy barrier has been chosen as the representative rate. (The additional molecules present in the cluster might conceivably also affect the reaction rate, which was neglected in the present study.)

The collision rate coefficient $\beta_{i,j}$ between clusters i and j were calculated using hard-sphere collision theory[58]:

$$\beta_{i,j} = \pi(r_i + r_j)^2 \sqrt{\frac{8k_BT}{\pi\mu}}, \tag{2}$$

where r_i is the radius of cluster i given by the Multiwfn 3.3.8 program[53], k_B is the Boltzmann constant, T is the temperature and $\mu = m_i m_j/(m_i + m_j)$ is the reduced mass. The cluster radius is half of the sum of the distance between the center of most distant atoms in cluster given by the Multiwfn 3.3.8 program[53] and the Van der Walls radii of these atoms.

Evaporation coefficients, $\gamma_{(i+j)\to i}$, were obtained from the corresponding collision coefficients and the Gibbs free energies of cluster formation using

$$\gamma_{(i+j)\to i} = \beta_{i,j} \frac{p_{ref}}{k_BT} \exp\left(\frac{\Delta G_{i+j} - \Delta G_i - \Delta G_j}{k_BT}\right), \tag{3}$$

where p_{ref} is the reference pressure (in this case 1 atm) at which the formation free energies were calculated, and ΔG_{i+j} is the Gibbs free energy of formation of cluster $i+j$ from monomers i and j.

The forward and reverse reaction rate coefficients of the chemical reaction were calculated according to the corresponding forward and reverse Gibbs free energy barrier using Eyrings

equation as[59]

$$k = \frac{k_\mathrm{B}T}{h} e^{-\frac{\Delta G^{\ddagger}}{RT}}, \tag{4}$$

where k_B is Boltzmann's constant, h is Planck's constant, and $\Delta \mathrm{G}^{\ddagger}$ is the Gibbs free energy of activation. The Gibbs free energy barrier and rate constants of the forward and reverse reactions are shown in Tables S1-S2 of the supplementary material.[34]

In addition, the tunneling effects could enhance the rate of chemical reaction involving hydrogen atom transfer especially at low temperatures.[60] Thus, the effect of tunneling on the hydration reaction is considered to correct the corresponding reaction rate constant through the Wigner tunneling correction by a factor $\Gamma(T)$ as

$$\Gamma(T) = 1 + \frac{1}{24} \left(\frac{h \nu^{\mp}}{k_B T} \right)^2, \tag{5}$$

where h is the Planck's constant, k_B is Boltzmann's constant, T is the temperature and $\nu^{\mp}$ is the imaginary frequency of the transition state.

Then, the Wigner tunneling factor corrected forward and reverse reaction rate coefficients $(k_{i \to j}, k_{j \to i})$ of the chemical reaction can be calculated by the tunneling facter as

$$k_{\mathrm{cor}} = \Gamma k. \tag{6}$$

The data of $\Gamma(T)$ of all hydration reactions in the present study at different temperatures (220, 240, 260, 280 and 300 K) are listed in Table S3 of the supplementary material. It indicates that the maximum value of the $\Gamma(T)$ among all the reactions of the present study is 4.34 (the uncatalyzed hydration reaction) at 220 K, which indicates that the tunneling effect has relatively small influence on the present study. The final hydraton reaction rate

8

132 coefficients are still corrected by the Wigner tunneling factor (Table S4 of the supplementary

133 material) to make the results more accurate.

134   Atmospheric clusters of hygroscopic species are almost invariably hydrated because the

135 concentration of water in the atmosphere is much larger than that of other condensable

136 species. All the hydrated clusters in the studied system with a relative population of higher

137 than 5% are considered. Further, the effective collision and evaporation coefficients of clus-

138 ters need to be computed as a weighted average over the hydrate distributions to get the

139 effective collision and evaporation coefficients.

140   The hydrate distributions for a cluster $\mathbf{C}$ were calculated as[61]

$$f(\mathbf{CW}_i) = \frac{[\mathbf{CW}_i]}{\sum_{j=0}^{j_{\max}} [\mathbf{CW}_j]}, \tag{7}$$

142 where $\mathbf{C}$ is a dry molecule or cluster other than water, $\mathbf{W}$ is water, $\mathbf{CW}_i$ is the cluster

143 consisting of $\mathbf{C}$ and i water molecules, and $[\mathbf{CW}_i]$ is the concentration of cluster $\mathbf{CW}_i$.

$$\frac{[\mathbf{CW}_i]}{[\mathbf{C}]} = \left([\mathbf{W}]\frac{k_B T}{p_{ref}}\right)^i \exp\left(\frac{\Delta G(\mathbf{C}) - \Delta G(\mathbf{CW}_i)}{k_B T}\right), \tag{8}$$

145 where $[\mathbf{W}]$ is the concentration of water vapor and p_{ref} is the reference pressure (in this

146 case 1 atm) at which the Gibbs free energies are calculated.

147   The effective collision coefficients were calculated as

$$\beta_{eff}(\mathbf{C} + \mathbf{D}) = \sum_{i=0}^{i_{\max}} \sum_{j=0}^{j_{\max}} \beta(\mathbf{CW}_i + \mathbf{DW}_j) f(\mathbf{CW}_i) f(\mathbf{DW}_j), \tag{9}$$

9

the effective evaporation coefficients similarly as

$$\gamma_{eff}\left(\mathbf{CD} \rightarrow \mathbf{C} + \mathbf{D}\right) = \sum_{i=0}^{i_{\max}} \sum_{j=0}^{j_{\max}} \gamma\left(\mathbf{CDW}_{i+j} \rightarrow \mathbf{CW}_i + \mathbf{DW}_j\right) f\left(\mathbf{CDW}_{i+j}\right), \qquad (10)$$

and the reaction rate coefficient as

$$k_{eff}(\mathbf{C} \rightarrow \mathbf{D}) = \sum_{i=1}^{i_{\max}} k_{\mathrm{cor}}\left(\mathbf{CW}_i \rightarrow \mathbf{DW}_{i-1}\right) f\left(\mathbf{CW}_i\right). \qquad (11)$$

Thus, when considering the presence of water, the birth-death equations can be written as

$$\begin{aligned}
\frac{dc_i}{dt} =& \frac{1}{2}\sum_{j<i} \beta_{eff\,j,(i-j)} c_j c_{(i-j)} + \sum_j \gamma_{eff\,(i+j)\rightarrow i} c_{i+j} - \sum_j \beta_{eff\,i,j} c_i c_j \\
& -\frac{1}{2}\sum_{j<i} \gamma_{eff\,i\rightarrow j} c_i + \sum_j k_{eff\,j\rightarrow i} c_j - \sum_j k_{eff\,i\rightarrow j} c_i + Q_i - S_i.
\end{aligned} \qquad (12)$$

The concentration of sulfuric acid **SA**, **A** and **GA** are set in the range of $1.0 \times 10^4 \sim 1.0 \times 10^8$ molecules cm^{-3},[62–65] $1.0 \times 10^7 \sim 1.0 \times 10^{11}$ molecules cm^{-3},[62] and $1.0 \times 10^7 \sim 1.0 \times 10^{11}$ molecules cm^{-3},[32,66–68] respectively, which are relevant to the corresponding common atmospheric concentration. The water vapour concentration was adjusted depending on the temperature according to the study on the saturation vapor pressure from Arnold Wexler.[69] The model runs were performed in the temperature range from 220K to 300K representing the range from the ground level to the upper free troposphere and RH ranged from 0 to 100%.

The boundary conditions require the outgrowing clusters to have a favorable composition so that the clusters leaving the studied size range are stable enough not to evaporate back immediately. $(\mathbf{SA})_3 \cdot \mathbf{A}_1$ cluster, with a maximum evaporation rate coefficient of 55 s^{-1} at
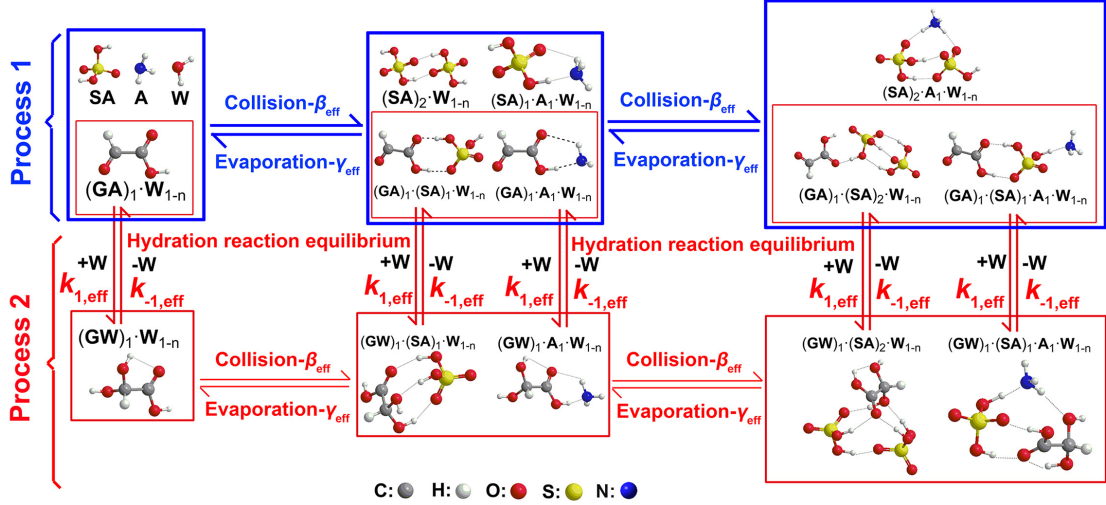
FIG. 1. Modeled clustering processes involving the hydration reaction of **GA** and **GA/GW**-based clusters. Process 1 (formation of **GA**-based clusters) and process 2 (formation of **GW**-based clusters) are shown in the blue and red line frame, respectively. For simplicity, water molecules in the cluster structures are not shown.

168 300 K, is relatively stable enough to resist evaporation (the evaporation rate coefficients of

169 clusters are shown in Table S5 of the supplementary material). Thus, the boundary condition

170 was set to be the $(\mathbf{SA})_3 \cdot \mathbf{A}_1$ cluster (see section 2 in the supplementary material for details).

171 It should be noted that using this relatively small cluster as a boundary condition might

172 overestimate absolute NPF rates, but it is probably sufficient for probing the relative effect

173 of **GA/GW** on cluster formation rate, which is the purpose of this study.

III.   RESULTS AND DISCUSSION

175   The clustering process of **GA**, involving the hydration reaction, includes two kinds of

176 processes (Figure 1). Process 1 is the formation of **GA**-**SA**-**A** containing clusters involving

177 only collision and evaporation steps (without chemical reactions). Process 2 involves not

178 only the collision and evaporation of **GW**-**SA**-**A** containing clusters, but also the hydration

179 reactions of **GA**-based clusters to form **GW**-based clusters.

11

A.   Structure and thermodynamic analysis

The clustering process of **GA** considering hydration reaction involves 35 different unhy-drated and hydrated clusters (Figures S1-S6 of the supplementary material). The cartesian coordinates of all clusters are listed in Tables S6-S83 of the supplementary material. The atoms in molecules (AIM) analyses were performed to search the bond critical points (BCPs), ring critical points (RCPs) and to calculate electron density ρ and Laplacian $\bigtriangledown^2\rho$ at the BCPs (Table S84 of the supplementary material). The AIM plots of the clusters without water molecules are shown in Figure S7 of the supplementary material. All these AIM results affirm the existence of intermolecular interaction in clusters. Moreover, the values of ρ and $\bigtriangledown^2\rho$ at these BCPs range from 0.0115 to 0.0927 a.u. and 0.0288 to 0.1815 a.u. respectively. Most of these values are larger than the critical threshold limits for the forma-tion of hydrogen bond suggested in the littrature (0.002-0.040 a.u. and 0.014-0.139 a.u. for $\rho(BCP)$ and $\bigtriangledown^2\rho(BCP)$, respectively).[70,71] These values of ρ and $\bigtriangledown^2\rho$ thus indicate quite strong hydrogen bond interactions. In addition, there is a large cluster rearrangement after the chemical reaction. The **GA** molecule binds preferentially to the periphery of the cluster (linear), almost solely by the interaction between its carboxyl group and sulfuric acid. After the reaction, both of the carboxyl group and the hydroxyl group of **GW** can interact with all the other clustering constituents inside the cluster (cage-like).

From the Gibbs free energies of formation of clusters (Figure S8 of the supplementary material), it can be seen that the clusters based on $(\mathbf{GA})_1 \cdot (\mathbf{SA})_1$ and $(\mathbf{GA})_1 \cdot (\mathbf{SA})_2$ are more stable than their corresponding **GW**-based analogues. In contrast, the hydrated clus-ters based on $(\mathbf{GW})_1 \cdot (\mathbf{SA})_1 \cdot \mathbf{A}_1$ are much more stable than their corresponding **GA**-based analogues at different temperatures.

B. Relative hydration population

GA and GW are both water soluble organics, and they can influence the hydrate distribution of clusters. The relative hydration population of clusters with varying numbers of water molecules at different relative humidities (20%, 40%, 60% and 100%) and moderate temperature of 260K are shown in Figure 2. The influence of GA and GW on the relative hydration population of clusters is different. The addition of GA on $(SA)_1 \cdot A_1$ cluster reduces the relative population of clusters with four water molecules and enhancing that of clusters without water molecules, and the addition of GA on $(SA)_2$ cluster reduces the relative population of clusters with three water molecules making the population more evenly. Thus, the addition of GA reduces the ability of $(SA)_1 \cdot A_1$ and $(SA)_2$ clusters to bind more water molecules. However, addition of GW on $(SA)_1 \cdot A_1$ cluster enhances the relative population of clusters with four water molecules reducing that of clusters without water molecules, and the addition of GW on $(SA)_2$ cluster enhances the relative population of clusters with five water molecules. Thus, the addition of GW enhances the ability of $(SA)_1 \cdot A_1$ and $(SA)_2$ clusters to bind more water molecules. This difference between the influence of GA and GW on the cluster hydration population can be explained from the structure characteristic and thermodynamic stability of the corresponding clusters. Two kinds of groups (carboxyl group and hydroxyl group) of GW can form hydrogen bonds, whereas only one group (carboxyl group) of GA participates in the hydrogen formation in the stable structures of clusters (Figures S1-S6 of the supplementary material). Moreover, the formation Gibbs free energies of the hydrated clusters involving GW with relatively high population are more negative than those involving GA.

Based on this result, the hydration reaction products of oxocarboxylic acids can be ex-

13
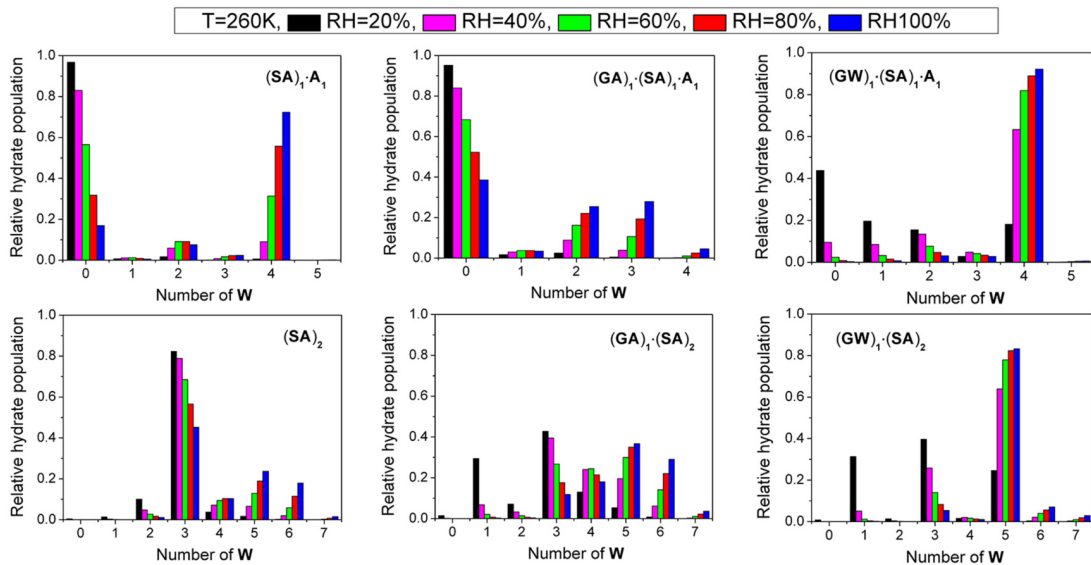
FIG. 2. Hydrate distributions of selected clusters at varying relative humidities at 260K.

pected to drastically increase the hygroscopicity of clusters.

C. The realistic hydration reaction conversion ratio of GA-based clusters

The hydration reaction in **GA**-based clusters can be uncatalyzed or catalyzed by **SA**, **W** or **A** as described in our previous study.[34] Which kind of hydration reaction occurs in a certain **GA**-based cluster depends on what kinds of molecules the cluster contains. Here, we assume that the reaction is always catalyzed by the most effective (lowest activation free energy barrier) catalyst present. In addition, clusters with different number of water molecules may have different hydration reaction pathways available. For example, no hydration reaction is possible for the $(\mathbf{GA})_1 \cdot (\mathbf{SA})_1$ cluster, but the **SA** catalyzed hydration reaction can occur in the $(\mathbf{GA})_1 \cdot (\mathbf{SA})_1 \cdot \mathbf{W}_1$ cluster. Therefore, two factors should be considered to calculate the realistic hydration reaction conversion ratio of **GA**-based clusters: one is the most effective catalysis mechanism, and the other is the relative population of the corresponding cluster. Thus, the rate constants corresponding to the catalyst with the low-

14
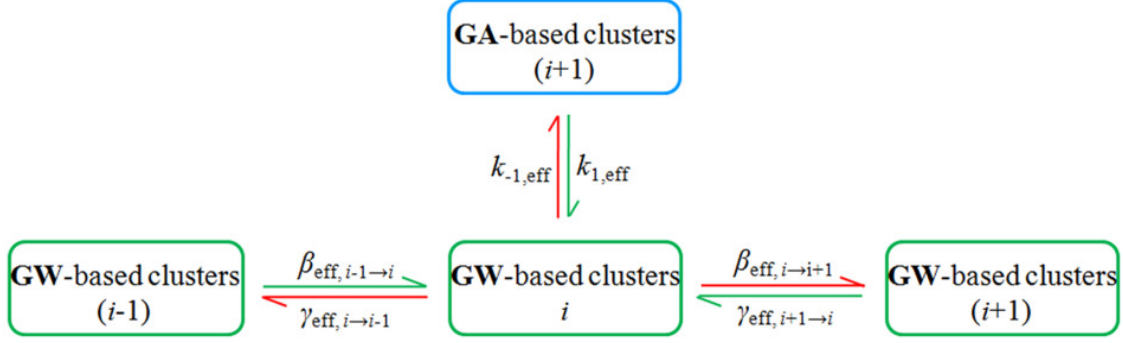
FIG. 3. The source (shown as green arrows) and sink (shown as red arrows) of **GW**-based clusters. Index i indicates the number of the molecules in the cluster. The hydrate distribution has been considered in the effective collisions rates β_{eff}, evaporation rates γ_{eff} and reaction rates k_{eff}. k_{eff} corresponds to the most effective catalyst for the hydration reaction, the nature of which depends on the composition of the cluster.

est activation free energy are weighted by the hydrate distribution. The **GW**-based clusters with i molecules in Figure 3 can be formed by the collision of the smaller **GW**-based clusters containing i-1 molecules and the evaporation of the bigger **GW**-based clusters containing i+1 molecules. In addition, they can be formed directly from the hydration reaction of **GA**-based clusters with i+1 molecules.

The hydration conversion ratio is one of the most important factors determining whether the hydration reaction should be considered in modelling NPF. The hydration reaction occurs either via collision of the two reactant molecules (**GA** and **W**), or in the clusters. Depending on the cluster composition, several different catalyzed processes may be possible.[34] The pathway with the lowest activation free energy barrier is always included in our process model (Figure 4).

The hydration conversion ratio ($X_{\mathbf{GA}}$) of **GA** in the studied system is defined as

$$X_{\mathbf{GA}}(\%) = \frac{\sum \left[(\mathbf{GW})_1 \cdot (\mathbf{SA})_y \cdot \mathbf{A}_z \cdot \mathbf{W}_n\right]}{\sum \left(\left[\left[(\mathbf{GA})_1 \cdot (\mathbf{SA})_y \cdot \mathbf{A}_z \cdot \mathbf{W}_n\right] + \left[(\mathbf{GW})_1 \cdot (\mathbf{SA})_y \cdot \mathbf{A}_z \cdot \mathbf{W}_n\right]\right]\right)} \times 100, \quad (13)$$
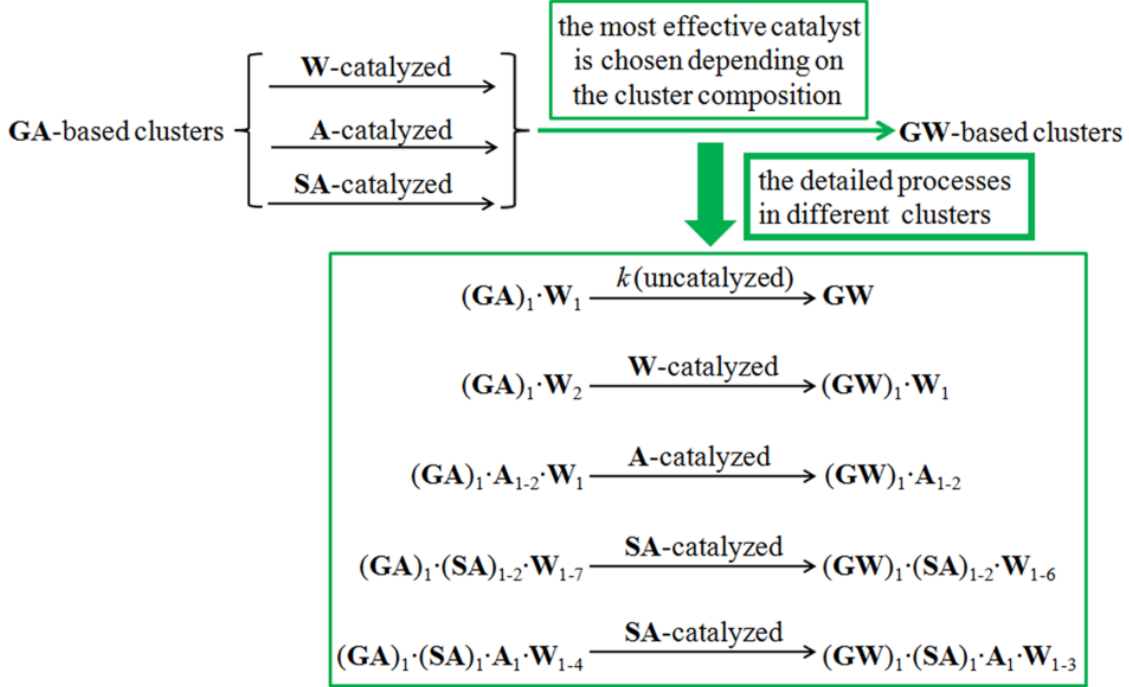
FIG. 4. Detailed information of the hydration reaction in clusters of the studied system.

where $[(\mathbf{GA/GW})_1 \cdot (\mathbf{SA})_y \cdot \mathbf{A}_z \cdot \mathbf{W}_n]$ is the concentration of $\mathbf{GA/GW}$-based clusters (or, for $y=0$, $z=0$ and $n=0$, $\mathbf{GA/GW}$ monomers). The denominator represents the sum of all $\mathbf{GA}$ or $\mathbf{GW}$ containing clusters (and monomers) in the system, and numerator represents the numbers of clusters where $\mathbf{GA}$ has been converted to $\mathbf{GW}$. We have modeled the conversion ratio $X_{\mathbf{GA}}$ under different atmospheric conditions (different conditions in Figure 5 are the chosen so that they correspond to the range of values in the atmosphere). The detailed values of the conversion ratios in different conditions are given in Tables S85-S86 of the supplementary material.

Figure 5 shows that in most atmospherically relevant conditions, the ammonia ($\mathbf{A}$) concentration has no effect on the conversion ratio ($X_{\mathbf{GA}}$), while the RH has a moderate effect. The surprisingly weak RH dependence is caused by a "saturation" of the water-catalyzed pathway already at fairly low RH values. In contrast, $X_{\mathbf{GA}}$ clearly increases with decreasing temperature (Figure 5(a)), and increases with increasing sulfuric acid ($\mathbf{SA}$) concentration
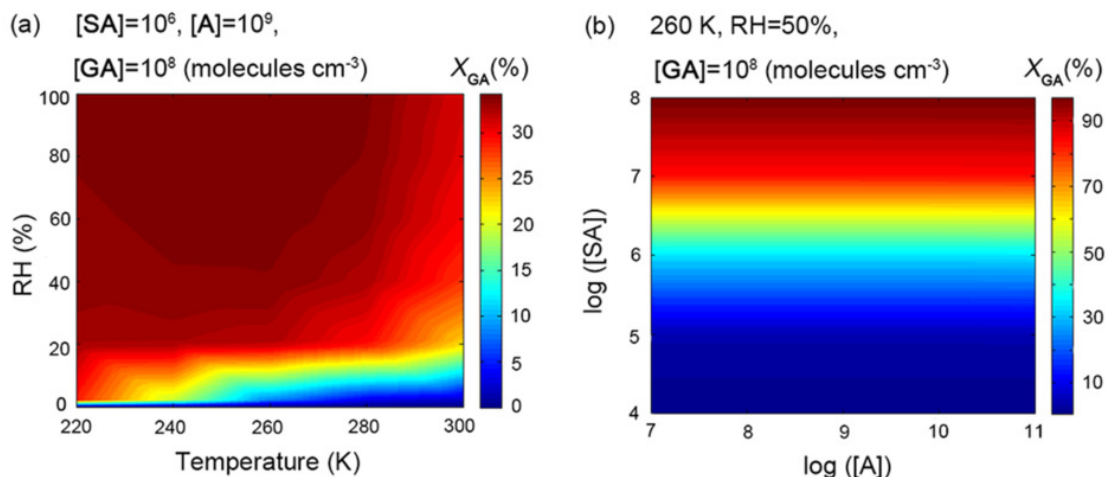
FIG. 5. The conversion ratio, $X_{\mathbf{GA}}$ (%), of glyoxylic acid (**GA**) hydration forming its geminal diol (**GW**) at varying (a) temperatures (K) and RHs (%) and (b) base-10 logarithm of the concentrations (molecules cm^{-3}) of **A** and **SA**. The color scales are shown on the right.

265 (Figure 5(b)). That is due to the fact that sulfuric acid catalyzes this reaction much more

266 effectively than ammonia or water.[34] $X_{\mathbf{GA}}$ is more than 50% when **SA** concentration is

267 more than 1.0×10^6 molecules cm^{-3}, and can reach up to 85% when the concentration of **SA**

268 is about 1.0×10^7 molecules cm^{-3} (Figure 5(b)). The relatively high conversion ratio could

269 significantly affect the relative abundances of oxocarboxylic acids and their corresponding

270 geminal diols and thus NPF, especially in the regions where **SA** is abundant, such as the

271 polluted regions and coastal areas.

272 **D.   Cluster formation rate**

273   A suitable measure for the enhancement of cluster formation rate (J) by **GA** and its

274 hydration reaction product (**GW**) is the comparison of the cluster formation rate involving

275 both **GA** and **GW** with that of **SA**-**A**-based clusters under similar conditions, i.e.

276
$$r_1 = \frac{J\left([\mathbf{GA}+\mathbf{GW}]=x,[\mathbf{SA}]=y,[\mathbf{A}]=z\right)}{J\left([\mathbf{GA}]=0,[\mathbf{SA}]=y,[\mathbf{A}]=z\right)}, \tag{14}$$

17

₂₇₇ where r_1 is the enhancement factor, $J([\mathbf{GA+GW}]=x],[\mathbf{SA}=y,[\mathbf{A}]=z)$ represents the forma-

₂₇₈ tion rate of $(\mathbf{GA/GW})_x{\cdot}(\mathbf{SA}){\cdot}_y\mathbf{A}_z$ clusters with variable numbers of water molecules (and

₂₇₉ including the effect of $\mathbf{GA}$ hydration reactions), and $J([\mathbf{GA}]=0,[\mathbf{SA}]=x,[\mathbf{A}]=y])$ reprensents

₂₈₀ the formation rate of the corresponding clusters without $\mathbf{GA}$ or $\mathbf{GW}$.

₂₈₁   As shown in Figure 6 (a, b, c), the enhancement factor r_1 is greater than 1, which indi-

₂₈₂ cates that $\mathbf{GA}$ can enhance the $\mathbf{SA}$-$\mathbf{A}$-based cluster formation rate. r_1 increases with the

₂₈₃ increase of $\mathbf{GA}$ concentrations, and but only becomes significant when the temperature is

₂₈₄ lowered to 220K. Thus, the influence of relative humidity, sulfuric acid ($\mathbf{SA}$) concentration

₂₈₅ and ammonia ($\mathbf{A}$) concentration on the cluster formation rate were studied at 220K. The

₂₈₆ enhancement is relatively large at high RH, low $\mathbf{SA}$ concentrations and high $\mathbf{A}$ concentra-

₂₈₇ tions. The enhancement factor exceeds 10 when the $\mathbf{SA}$ concentration lower than $1.0 \times$

₂₈₈ 10^6 molecules cm^{-3}, and a high $\mathbf{A}$ concentration of 1.0×10^{11} molecules cm^{-3}, at which

₂₈₉ the absolute formation rate of $\mathbf{GA}$-$\mathbf{SA}$-$\mathbf{A}$-based clusters is as high as 2.77×10^4 cm^{-3} s^{-1}

₂₉₀ (the absolute formation rates of $\mathbf{GA}$-$\mathbf{SA}$-$\mathbf{A}$-based clusters at different temperatures, RHs

₂₉₁ and concentrations of $\mathbf{GA}$, $\mathbf{SA}$ and $\mathbf{A}$ are listed in Tables S87-S89 of the supplementary

₂₉₂ material). When the $\mathbf{SA}$ concentration is low, and the $\mathbf{A}$ concentration high, there will be

₂₉₃ enough $\mathbf{A}$ to cluster with $\mathbf{GA}$ and $\mathbf{GW}$ despite the stronger binding between $\mathbf{SA}$ and $\mathbf{A}$

₂₉₄ compared to $\mathbf{GA/GW}$ and $\mathbf{A}$.

₂₉₅   To assess the significance of the hydration reaction of $\mathbf{GA}$, we compared the cluster

₂₉₆ formation with $\mathbf{GA}$ present, but both with and without hydration reaction (Figure 7). A

₂₉₇ suitable measure for the effect of the hydration reaction is the ratio of formation rates in

₂₉₈ the case where the hydration reaction of $\mathbf{GA}$ to form $\mathbf{GW}$ is allowed to the rate in the case

₂₉₉ when this reaction is not occurring:

<div align="center">18</div>
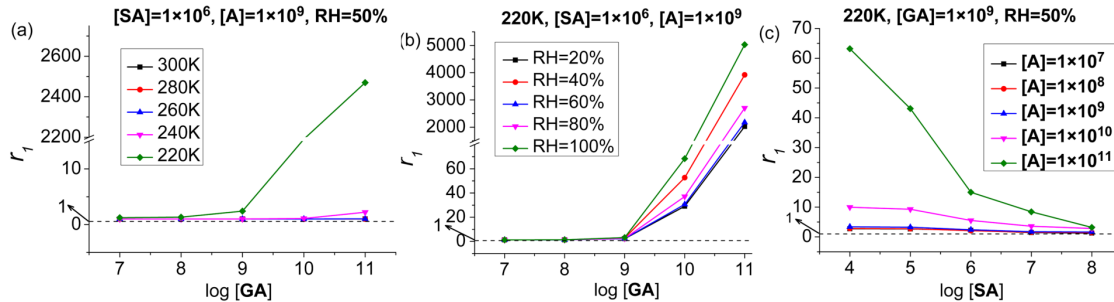
FIG. 6. Enhancement of **SA**-**A**-**W** cluster formation rate due to **GA** and **GW** as a function of the conditions (concentrations, molecules cm^{-3}) (Eq. 14).

$$r_2 = \frac{J\left([\mathbf{GA} + \mathbf{GW}] = x, [\mathbf{SA}] = y, [\mathbf{A}] = z\right)}{J\left([\mathbf{GA}] = x, [\mathbf{SA}] = y, [\mathbf{A}] = z\right)}, \tag{15}$$

where $J\left([\mathbf{GA}=x,[\mathbf{SA}]=y,[\mathbf{A}]=z]\right)$ indicates the cluster formation rate in a system involving **GA** but not allowing the hydration reaction.

The common trend is that r_2 increases with increasing of **GA** concentrations, but is not significant until the temperature is lowered to 220K (Figure 7 (a)). Thus, the influence of relative humidity, sulfuric acid (**SA**) concentration and ammonia (**A**) concentration on the cluster formation rate were studied at 220K. The effect of hydration reactions on NPF is more significant at high RH, low sulfuric acid (**SA**) concentration and high ammonia (**A**) concentration. The likely explanation for this is that when **SA** concentration is low and the **A** concentration high, there will be enough **A** for **GA** and **GW** regardless of the stronger combination between **SA** and **A**. This makes the competition between **GA** and **GW** more pronounced, enhancing the ratio between cluster formation rates with hydration switched "on" and "off". Thus, both the effect of **GA** and its hydration reaction are most significant in cold, humid and relatively clean environments with little sulfuric acid, or agricultural regions polluted with ammonia.
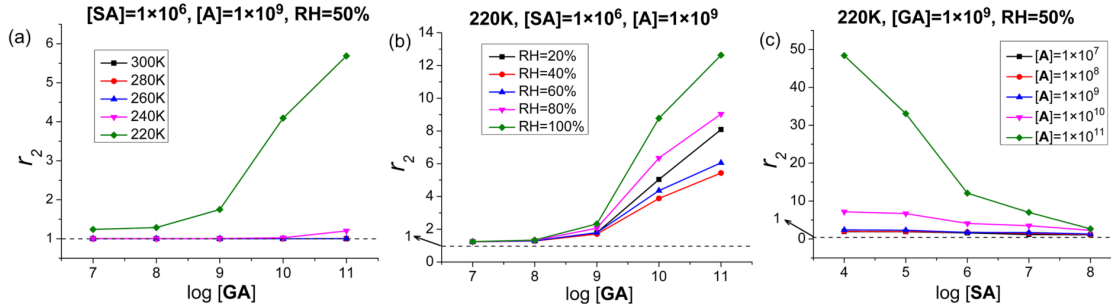
FIG. 7. Cluster formation rate involving **GA** and its hydration reaction relative to that involving **GA** but not its hydration reaction (Eq. 15).

E.   Cluster formation pathway

The main cluster formation pathways involving the hydration reaction of **GA** to form **GW** have been further studied at 220K (Figure 8). The flux through the system proceeds principally via two clustering mechanisms: one involves pure **SA**-**A**-clusters, and the other involves one **GA** or **GW** molecule in addition to **SA** and **A**. The clusters grow out of the size region studied through the addition of sulfuric acid to $(\mathbf{SA})_2 \cdot \mathbf{A}_1$ clusters. **GA**-based clusters easily form **GW**-based clusters through hydration reactions, for example converting $(\mathbf{GA})_1 \cdot (\mathbf{SA})_1 \cdot \mathbf{W}_n$ to $(\mathbf{GW})_1 \cdot (\mathbf{SA})_1 \cdot \mathbf{W}_{n-1}$. Though **GA** and **GW** evaporate easily from clusters from the point of view of the cluster stability, the contribution of **GW** to the formation of $(\mathbf{SA})_2$ or $(\mathbf{SA})_1 \cdot \mathbf{A}_1$ clusters can still reach up to 77% and 100%, respectively, due to the high concentration of **GA** and the high hydration conversion ratio combined with the thermodynamic stability. At the conditions corresponding to high R values, nearly 100% of the $(\mathbf{SA})_2 \cdot (\mathbf{A})_1$ clusters are formed via $(\mathbf{GW})_1 \cdot (\mathbf{SA})_1 \cdot \mathbf{A}_1$ clusters (Figure S9 of the supplementary material). Thus, the contribution of **GA** to **SA**-**A** NPF is potentially of great significance especially in the regions where the hydration conversion ratio is large.

20
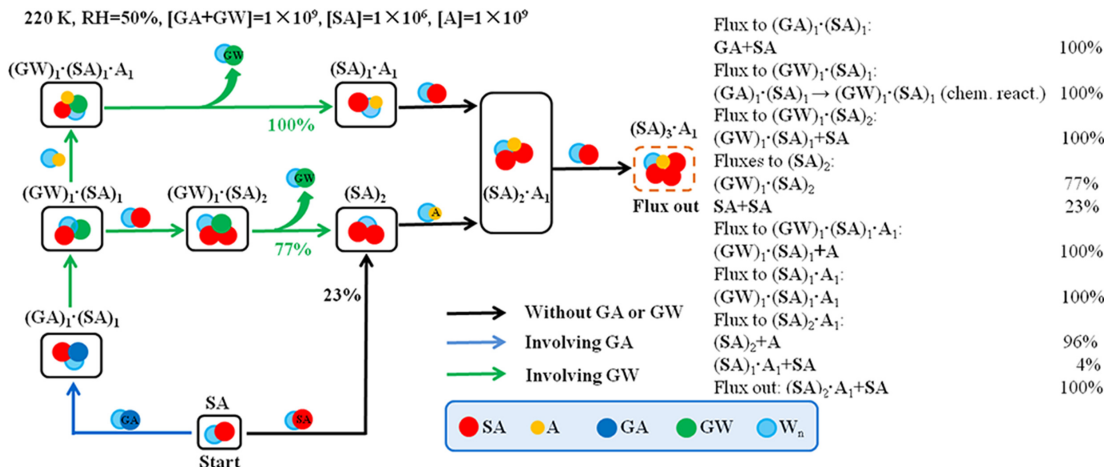
FIG. 8. Main cluster formation pathways considering the hydration reaction of **GA** forming **GW** are represented by arrows. Relative amounts of clusters formed via dominating growth pathways are indicated in the side table.

IV. CONCLUSIONS

The clustering mechanism involving hydration reaction of glyoxylic acid, as a representative example of oxocarboxylic acids, has been studied using Density Functional Theory combined with the Atmospheric Clusters Dynamic Code. Hydration reaction induces the difference in cluster structures, and the hydration reaction products of glyoxylic acid can drastically increase the hygroscopicity of clusters. In atmospheric conditions, the total hydration reaction conversion ratio of glyoxylic acid to its product (2,2-dihydroxyacetic acid) in both gas phase and clusters can be up to 85%, and the product can further participate in the clustering process. Thus, it can be speculated that the relatively high conversion ratio could significantly affect the relative abundances of oxocarboxylic acids and their corresponding geminal diols and thus NPF.

Neglecting the hydration reaction can thus induce a significant error in cluster formation rates and pathways, especially at relatively low temperature. In addition, the evaporation rates of larger oxocarboxylic acids (and especially their germinal diols) can be expected to

21

be lower due to more H-bonding groups and higher molecular weights. They are thus likely to participate in the cluster formation also at higher temperatures. Thus, the hydration reaction of oxocarboxylic acids in clustering process may be of greater importance in the atmosphere. A more general inference from the present study is that the hydration reactions of oxocarboxylic acids catalyzed by clustering with sulfuric acid and ammonia can increase both the hydroscopicity and stability of clusters, and thus contribute to NPF. The present study can provide a clearer picture of the effect mechanism of oxocarboxylic acids in NPF and indicates the prospect of nucleation process involving chemical reactions, which has significant implications for the improvement of the atmospheric models.

V. SUPPLEMENTARY MATERIAL

See supplementary material for the the Gibbs free energy barrier (kcal/mol) and the reaction rate constants (ref. 34), the Wigner tunneling correction factor and the tunneling effect factor corrected reaction rate constants for hydration reactions of **GA** with **W** (a) uncatalyzed, (b) catalyzed by **W**, (c) catalyzed by **SA** and (d) catalyzed by **A** at varying temperatures ranging from 220 K to 300 K, evaporation rate coefficients of clusters, cartesian coordinates of all clusters, AIM topological parameters for the stable clusters, the realistic hydration reaction conversion ratio ($X_{\mathbf{GA}}$), formation rates of clusters, the most stable configuration of the studied clusters, the AIM plots of the unhydrated clusters, Gibbs free energies of formation of clusters, the main cluster formation pathways considering the hydration reaction of **GA** forming **GW**, details for the boundary conditions and complete Gaussian 09 reference (Ref. 52)

ACKNOWLEDGMENTS

REFERENCES

[1] K. K. Ding, X. T. Kong, J. P. Wang, L. P. Lu, W. F. Zhou, T. J. Zhan, C. L. Zhang, and S. L. Zhuang, Environ. Sci. Technol. Lett. **51**, 6452 (2017).

[2] A. G. Rincón, M. I. Guzmán, M. R. Hoffmann, and A. J. Colussi, J. Phys. Chem. A **113**, 10512 (2009).

[3] C. L. Heald, D. J. Jacob, R. J. Park, L. M. Russell, B. J. Huebert, J. H. Seinfeld, H. Liao, and R. J. Weber, Geophys. Res. Lett. **32**, L18809 (2005).

[4] R. Volkamer, J. L. Jimenez, F. S. Martini, K. Dzepina, Q. Zhang, D. Salcedo, L. T. Molina, D. R. Worsnop, and M. J. Molina, Geophys. Res. Lett. **33**, L17811 (2006).

[5] R. Y. Zhang, I. Suh, J. Zhao, D. Zhang, E. C. Fortner, X. X. Tie, L. T. Molina, and M. J. Molina, Science **304**, 1487 (2004).

[6] R. Y. Zhang, A. Khalizov, L. Wang, M. Hu, and W. Xu, Chem. Rev. **112**, 1957 (2012).

[7] H. L. Zhao, Q. Zhang, and L. Du, RSC Adv. **6**, 71733 (2016).

[8] Q. Zhang and L. Du, Comput. Theor. Chem. **1078**, 123 (2016).

[9] I. K. Ortega, N. M. Donahue, T. Kurtén, M. Kulmala, C. Focsa, and H. Vehkamäki, J. Phys. Chem. A **120**, 1452 (2016).

[10] J. Elm, N. Myllys, T. Olenius, R. Halonen, T. Kurtén, and H. Vehkamäki, Phys. Chem. Chem. Phys. **19**, 4877 (2017).

[11] H. B. Xie, J. Elm, R. Halonen, N. Myllys, T. Kurtén, M. Kunlmala, and H. Vehkamäki, Environ. Sci. Technol. **51**, 8422 (2017).

[12] C. Chirs, Nature **533**, 478 (2016).

[13] S. Li, K. Qu, H. Zhao, L. Ding, and L. Du, Chem. Phys. **472**, 198 (2016).

23

392 [14]H. L. Zhao, S. S. Tang, S. Y. Li, L. Ding, and L. Du, Struct. Chem **27**, 1241 (2016).

393 [15]J. Elm, M. Passananti, T. Kurtén, and H. Vehkamäki, J. Phys. Chem. A **121**, 6155 (2017).

394 [16]S. Guo, M. Hu, M. L. Zamora, J. F. Peng, D. J. Shang, J. Zheng, Z. F. Du, Z. J. Wu,

395 M. Shao, L. M. Zeng, M. J. Molina, and R. Y. Zhang, Proc. Natl. Acad. Sci. U. S. A.

396 **111**, 17373 (2014).

397 [17]N. Zhao, Q. Z. Zhang, and W. X. Wang, Sci. Total Environ. **563-564**, 1008 (2016).

398 [18]J. Dang, X. L. Shi, Q. Z. Zhang, and W. X. Wang, Sci. Total Environ. **517**, 1 (2015).

399 [19]X. W. Wang, B. Jing, F. Tan, J. B. Ma, Y. H. Zhang, and M. F. Ge, Atmos. Chem. Phys.

400 **17**, 12797 (2017).

401 [20]V. Hirvonen, N. Myllys, T. Kurtén, and J. Elm, J. Phys. Chem. A **122**, 1771 (2018).

402 [21]H. B. Xie, F. F. Ma, Y. Q., and C. J. W., J. Phys. Chem. A **121**, 1657 (2017).

403 [22]J. Liu, S. Fang, Z. Wang, W. Yi, F.-M. Tao, and J. Y. Liu, Environ. Sci. Technol. **49**,

404 13112 (2015).

405 [23]J. J. Liu, S. Fang, W. Liu, M. Y. Wang, F. M. Tao, and J. Y. Liu, J. Phys. Chem. A **119**,

406 102 (2015).

407 [24]X. Shi, R. Zhang, Y. Sun, X. F., Q. Zhang, and W. Wang, Phys. Chem. Chem. Phys. **20**,

408 1005 (2018).

409 [25]T. Kurtén, J. Elm, N. L. Prisle, K. V. Mikkelsen, C. J. Kampf, E. M. Waxman, and

410 R. Volkamer, J. Phys. Chem. A **119**, 4509 (2015).

411 [26]M. Shrivastava, C. D. Cappa, J. Fan, A. H. Goldstein, A. B. Guenther, J. L. Jimenez,

412 C. Kuang, A. Laskin, S. T. Martin, N. L. Ng, T. Petaja, J. R. Pierce, P. J. Rasch,

413 P. Roldin, J. H. Seinfeld, J. Shilling, J. N. Smith, J. A. Thornton, R. Volkamer, J. Wang,

414 D. R. Worsnop, R. A. Zaveri, A. Zelenyuk, and Q. Zhang, Rev. Geophys. **55**, 509 (2017).

415 [27]K. L. Plath, J. L. Axson, G. C. Nelson, K. Takahashi, R. T. Skodje, and V. Vaidaa, React.

416 Kinet. Catal. Lett. **96**, 209 (2009).

417 [28]J. L. Axson, K. Takahashi, D. O. D. Haan, and V. Vaida, Proc. Natl. Acad. Sci. U. S. A.

418 **107**, 6687 (2010).

419 [29]M. K. Hazra, J. S. Francisco, and A. Sinha, J. Phys. Chem. A **117**, 11704 (2013).

420 [30]M. K. Hazra, J. S. Francisco, and A. Sinha, J. Phys. Chem. A **118**, 4095 (2014).

421 [31]R. J. Weber, J. J. Marti, P. H. McMurry, F. L. Elsele, D. J. Tanner, and A. Jefferson,

422 Chem. Eng. Commun. **151**, 53 (1996).

423 [32]R. Ortiz, K. Enya, K. Sekiguchi, and K. Sakamoto, Atmos. Environ. **43**, 382 (2009).

[424] [33]G. H. Wang, K. Kawamura, C. L. Cheng, J. J. Li, J. J. Cao, R. J. Zhang, T. Zhang, S. X.
[425] Liu, and Z. Z. Zhao, Environ. Sci. Technol. **46**, 4783 (2012).

[426] [34]L. Liu, X. H. Zhang, Z. S. Li, Y. H. Zhang, and M. F. Ge, Chemosphere **186**, 430 (2017).

[427] [35]M. J. McGrath, T. Olenius, I. K. Ortega, V. Loukonen, P. Paasonen, T. Kurtén, M. Kul-
[428] mala, and H. Vehkamäki, Atmos. Chem. Phys. **12**, 2345 (2012).

[429] [36]H. Henschel, J. C. A. Navarro, T. Yli-Juuti, O. Kupiainen-Määttä, T. Olenius, I. K.
[430] Ortega, S. L. Clegg, T. Kurtén, I. Riipinen, and H. Vehkamäki, J. Phys. Chem. A **118**,
[431] 2599 (2014).

[432] [37]J. Zhang and M. Dolg, Phys. Chem. Chem. Phys. **17**, 24173 (2015).

[433] [38]J. Zhang and M. Dolg, Phys. Chem. Chem. Phys. **18**, 3003 (2016).

[434] [39]A. D. M. Jr., D. Bashford, M. Bellott, J. R. L. Dunbrack, J. D. Evanseck, M. J. Field,
[435] S. Fischer, J. Gao, H. Guo, S. Ha, D. Joseph-McCarthy, L. Kuchnir, K. Kuczera, F. T. K.
[436] Lau, C. Mattos, S. Michnick, T. Ngo, D. T. Nguyen, B. Prodhom, W. E. R. III, B. Roux,
[437] M. Schlenkrich, J. C. Smith, R. Stote, J. Straub, M. Watanabe, J. Wiórkiewicz-Kuczera,
[438] D. Yin, and M. Karplus, J. Phys. Chem. B **102**, 3586 (1998).

[439] [40]J. J. P. Stewart, J. Mol. Model. **13**, 1173 (2007).

[440] [41]J. J. P. Stewart, J. Mol. Model. **19**, 1 (2013).

[441] [42]J. J. P. Stewart, Colorado Springs, CO, USA.

[442] [43]Y. Zhao and D. G. Truhlar, Theor. Chem. Acc. **120**, 215 (2008).

[443] [44]Y. Zhao and D. G. Truhlar, Chem. Phys. Lett. **502**, 1 (2011).

[444] [45]M. J. Frisch, J. A. Pople, and J. S. Binkley, Chem. Phys. Lett. **80**, 3265 (1984).

[445] [46]J. Elm, M. Bilde, and K. V. Mikkelsen, J. Chem. Theory Comput. **8**, 2071 (2012).

[446] [47]J. Elm, M. Bilde, and K. V. Mikkelsen, Phys. Chem. Chem. Phys. **15**, 16442 (2013).

[447] [48]J. Herb, A. B. Nadykto, and F. Q. Yu, Chem. Phys. Lett. **518**, 7 (2011).

[448] [49]A. B. Nadykto, F. Yu, M. V. Jakovleva, J. Herb, and Y. Xu, Entropy **13**, 554 (2011).

[449] [50]A. B. Nadykto, F. Yu, and J. Herb, Atmos. Chem. Phys. **9**, 4031 (2009).

[450] [51]J. Herb, Y. Xu, F. Yu, and A. B. Nadykto, J. Phys. Chem. A **117**, 133 (2013).

[451] [52]M. J. Frisch, G. W. Trucks, and H. B. S. et al., Gaussian 09, Revision A.1 , Gaussian Inc.
[452] Wallingford CT (see SI for details) (2009).

[453] [53]T. Lu and F. Chen, J. Comput. Chem. **33**, 580 (2012).

[454] [54]T. Olenius, o. Kupiainen-Määttä, I. K. Ortega, T. Kurtén, and H. Vehkamäki, J. Chem.
[455] Phys. **139**, 084312 (2013).

[55] L. F. Shampine and M. W. Reichelt, Siam Journal on Scientific Computing **18**, 1 (1997).

[56] N. Bork, J. Elm, T. Olenius, and Vehkamäki, Atmos. Chem. Phys. **14**, 12023 (2014).

[57] M. Kulmala, M. Dal Maso, M. J. M., L. Pirjola, M. Väkevä, P. Aalto, P. Miikkulainen, and C. D. Hämeri, K. O'dowd, Tellus B **53**, 479490 (2001).

[58] J. H. Seinfel and S. N. Pandis, *Atmospheric chemistry and physics: from air pollution to climate change* (John Wiley & Sons, Inc., New York, 2006).

[59] H. Eyring, J. Chem. Phys. **3**, 107 (1935).

[60] M. Kumar, J. M. Anglada, and J. S. Francisco, J. Phys. Chem. A **121**, 43184325 (2017).

[61] T. Kurtén, M. Noppel, H. Vehkamäeki, M. Salonen, and M. Kulmala, Boreal Environ. Res. **12**, 431 (2007).

[62] I. Riipinen, S. L. Sihto, M. Kulmala, F. Arnold, M. Dal Maso, W. Birmili, K. Saarnio, K. Teinila, V. M. Kerminen, and A. Laaksonen, Atmos. Chem. Phys. **7**, 1899 (2007).

[63] J. Almeida, S. Schobesberger, A. Kürten, I. K. Ortega, O. Kupiainen-Määttä, A. P. Praplan, A. Adamov, A. Amorim, F. Bianchi, M. Breitenlechner, A. David, J. Dommen, N. M. Donahue, A. Downard, E. Dunne, J. Duplissy, S. Ehrhart, R. C. Flagan, A. Franchin, R. Guida, J. Hakala, A. Hansel, M. Heinritzi, H. Henschel, T. Jokinen, H. Junninen, M. Kajos, J. Kangasluoma, H. Keskinen, A. Kupc, T. Kurtén, A. N. Kvashin, A. Laaksonen, K. Lehtipalo, M. Leiminger, J. Leppä, V. Loukonen, V. Makhmutov, S. Mathot, M. J. McGrath, T. Nieminen, T. Olenius, A. Onnela, T. Petäjä, F. Riccobono, I. Riipinen, M. Rissanen, L. Rondo, T. Ruuskanen, F. D. Santos, N. Sarnela, S. Schallhart, R. Schnitzhofer, J. H. Seinfeld, M. Simon, M. Sipilä, Y. Stozhkov, F. Stratmann, A. Tomé, J. Tröstl, G. Tsagkogeorgas, P. Vaattovaara, Y. Viisanen, A. Virtanen, A. Vrtala, P. E. Wagner, E. Weingartner, H. Wex, C. Williamson, D. Wimmer, P. Ye, T. Yli-Juuti, K. S. Carslaw, M. Kulmala, J. Curtius, U. Baltensperger, D. R. Worsnop, H. Vehkamäki, and J. Kirkby, Nature **502**, 359 (2013).

[64] C. Kuang, P. H. Mcmurry, and F. L. Mccormick, Alon V.and Elsele, J. Geophys. Res. **113**, D10209 (2008).

[65] S. Schobesberger, H. Junninen, F. Bianchi, G. Lonn, M. Ehn, K. Lehtipalo, J. Dommen, S. Ehrhart, I. K. Ortega, A. Franchin, T. Nieminena, F. Riccobono, M. Hutterli, J. Duplissy, J. Almeida, A. Amorim, M. Breitenlechner, A. J. Downard, E. M. Dunne, R. C. Flagan, M. Kajos, H. Keskinen, J. Kirkby, A. Kupc, T. K. A. Kürten, A. Laaksonen, S. Mathot, A. Onnela, A. P. Praplan, L. Rondo, F. D. Santos, S. Schallhart,

R. Schnitzhofer, M. Sipilä, A. Tomé, H. V. G. Tsagkogeorgas, D. Wimmer, U. Baltensperger, K. S. Carslaw, J. Curtius, A. Hansel, T. Petäjä, M. Kulmala, N. M. Donahue, and D. R. Worsnop, Proc. Natl. Acad. Sci. U. S. A. **110**, 17223 (2013).

[66]B. Graham, O. L. MayolBracero, P. Guyon, G. C. Roberts, S. Decesari, M. C. Facchini, P. Artaxo, W. Maenhaut, P. Köll, and M. O. Andreae, J. Geophys. Res.: Atmos. **107**, 18047 (2002).

[67]W. Y. Zhao, K. Kawamura, S. Y. Yue, L. F. Wei, H. Ren, Y. Yan, M. Kang, L. J. Li, L. J. Ren, S. Lai, J. Li, Y. L. Sun, Z. F. Wang, and P. Q. Fu, Atmos. Chem. Phys. **18**, 2749 (2018).

[68]K. Kawamura, E. Tachibana, K. Okuzawa, S. G. Aggarwal, Y. Kanaya, and Z. F. Wang, Atmos. Chem. Phys. **13**, 8285 (2013).

[69]A. Wexler, J. Res. Natl. Bur. Stand. **80A**, 775 (1976).

[70]U. Koch and P. L. A. Popelier, J. Phys. Chem. **99**, 9747 (1995).

[71]U. Koch and P. L. A. Popelier, J. Phys. Org. Chem. **17**, 18 (2004).

Supplementary material for

Clustering Mechanism of Oxocarboxylic Acids Involving Hydration Reaction: Implications for the Atmospheric Models

Ling Liu,[a] Oona Kupiainen-Määttä,[b] Haijie Zhang,[a] Hao Li,[a] Jie Zhong[c], Theo Kurtén,[d] Hanna Vehkamäki,[b] Shaowen Zhang,[a] Yunhong Zhang,[a] Maofa Ge,[c] Xiuhui Zhang,[a*] Zesheng Li[a*]

[a] Key Laboratory of Cluster Science, Ministry of Education of China, School of Chemistry and Chemical Engineering, Beijing Institute of Technology, Beijing 100081, China

[b] Institute for Atmospheric and Earth System Research/Physics, University of Helsinki, PO Box 64 (Gustaf Hällströmin katu 2a), FI-00014, Helsinki, Finland

[c] Department of Chemistry, University of Nebraska-Lincoln, Lincoln, NE, USA 68588

[d] Institute for Atmospheric and Earth System Research/Chemistry, University of Helsinki, PO Box 64 (Gustaf Hällströmin katu 2a), FI-00014, Helsinki, Finland

[e] Beijing National Laboratory for Molecular Sciences (BNLMS), State Key Laboratory for Structural Chemistry of Unstable and Stable Species, Institute of Chemistry, Chinese Academy of Sciences, Beijing 100190, China

* E-mail: zhangxiuhui@bit.edu.cn (X. Zhang),
        zeshengli@bit.edu.cn (Z. Li).

Section 1. Tables and Figures

Table S1. The forward and reverse Gibbs free energy barrier (kcal/mol) for hydration reactions of **GA** with **W** (a) uncatalyzed, (b) catalyzed by **W**, (c) **SA** and (d) **A** relative to the corresponding pre-reactive clusters and the product clusters at varying temperatures ranging from 220 K to 300 K. (Ref. 1)

Table S2. The rate constants of the forward and reverse reactions, k_1 and k_{-1} (s^{-1}), respectively, for the hydration of **GA** with **W** (a) uncatalyzed, (b) catalyzed by **W**, (c) **SA** and (d) **A** at varying temperatures ranging from 220 K to 300 K. (Ref. 1)

Table S3. The imaginary frequencies (v_{im}, cm^{-1}) (Ref. 1) of the transition states (TSs) and the Wigner tunneling correction factor ($\Gamma(T)$) at different temperatures (220, 240, 260, 280 and 300 K) for hydration reactions of **GA** with **W** (a) uncatalyzed, (b) catalyzed by **W**, (c) **SA** and (d) **A** at M06-2X/6-311++G(3df,3pd) level of theory.

Table S4. The rate constants of the forward and reverse reactions ($k_{1,cor}$ and $k_{-1,cor}$(s^{-1})) corrected by the tunneling effect factor $\Gamma(T)$ according to Wigner at the different temperatures of 220, 240, 260, 280 and 300 K.

Table S5. The evaporation rate coefficients (s^{-1}) of all studied clusters at varying temperatures ranging from 220 K to 300 K.

Tables S6-S83. Cartesian coordinates of the studied clusters.

Table S84. AIM topological parameters for the stable clusters obtained at the M06-2X/6-311++G(3df,3pd) level (in a.u.).

Table S85. The realistic hydration reaction conversion ratio (X_{GA}, %) of GA-based clusters at varying temperatures and relative humidities.

Table S86. The realistic hydration reaction conversion ratio (X_{GA}, %) of GA-based clusters at varying ammonia and sulfuric acid concentrations.

Table S87. The formation rates (J, cm^{-3} s^{-1}) of $(\mathbf{GA/GW})_x \cdot (\mathbf{SA})_y \cdot \mathbf{A}_z$ clusters with the vabriations of the concentration of **GA** ([**GA**]) at different temperatures of 220, 240, 260, 280 and 300 K.

Table S88. The formation rates (J, cm^{-3} s^{-1}) of $(\mathbf{GA/GW})_x \cdot (\mathbf{SA})_y \cdot \mathbf{A}_z$ clusters with the vabriations of the concentration of **GA** ([**GA**]) at different relative humidities (RH) of 20%, 40%, 60%, 80% and 100%.

Table S89. The formation rates (J, cm^{-3} s^{-1}) of $(GA/GW)_x \cdot (SA)_y \cdot A_z$ clusters with the vabriations of the concentration of **SA** ([**SA**]) **and A** ([**A**]) at 220K.

Figures S1-S6. Most stable configuration of $(GA)_1 \cdot (SA)_1 \cdot W_n$ (n=0-3), $(GW)_1 \cdot (SA)_1 \cdot W_n$ (n=0-3), $(GA)_1 \cdot (SA)_2 \cdot W_n$ (n=0-6), $(GW)_1 \cdot (SA)_2 \cdot W_n$ (n=0-7), $(GA)_1 \cdot (SA)_1 \cdot N_1 \cdot W_n$ (n=0-4) and $(GW)_1 \cdot (SA)_1 \cdot N_1 \cdot W_n$ (n=0-5) clusters. The lengths of the hydrogen bonds are given in Å. The hydrogen bonds are shown as dashed lines.

Figure S8. Gibbs free energies (kcal mol^{-1}) of formation of clusters (a) $O_1 \cdot SA_1 \cdot W_n$, (b) $O_1 \cdot SA_2 \cdot W_n$ and (c) $O_1 \cdot SA_1 \cdot N_1 \cdot W_n$. **O** indicates **GA** or **GW**. The solid lines are to guide the eye.

Figure S9. Main cluster formation pathways considering the hydration reaction of **GA** forming **GW** are represented by arrows. Relative amounts of clusters formed via dominating growth pathways are indicated in the side table.

Section 2. Boundary Conditions

Complete Gaussian 09 reference (Reference 52)

Table S1. The forward and reverse Gibbs free energy barrier (kcal/mol) for hydration reactions of **GA** with **W** (a) uncatalyzed, (b) catalyzed by **W**, (c) **SA** and (d) **A** relative to the corresponding pre-reactive clusters and the product clusters at varying temperatures ranging from 220 K to 300 K. (Ref. 1)

Reactions	300 K	280 K	260 K	240 K	220 K
(a) forward	38.58	38.33	38.09	37.85	37.63
(a) reverse	44.87	44.82	44.78	44.73	44.69
(b) forward	23.98	23.66	23.34	23.05	22.77
(b) reverse	30.82	30.68	30.55	30.43	30.31
(c) forward	9.50	9.33	9.17	9.02	8.88
(c) reverse	17.97	17.95	17.92	17.90	17.88
(d) forward	22.90	22.70	22.50	22.31	22.13
(d) reverse	29.77	29.62	29.48	29.34	29.21

Table S2. The rate constants of the forward and reverse reactions, k_1 and k_{-1} (s^{-1}), respectively, for the hydration of **GA** with **W** (a) uncatalyzed, (b) catalyzed by **W**, (c) **SA** and (d) **A** at varying temperatures ranging from 220 K to 300 K. The unimolecular rate constants in this table are computed relative to the reactant or product clusters (e.g. **GA**-**W** in the case of the uncatalyzed reaction). (Ref. 1)

Temperatures	k_1 (a)	k_{-1} (a)	k_1 (b)	k_{-1} (b)	k_1 (c)	k_{-1} (c)	k_1 (d)	k_{-1} (d)
220	1.88×10^{-25}	1.83×10^{-32}	1.10×10^{-10}	3.54×10^{-18}	6.87×10^{3}	7.87×10^{-6}	4.70×10^{-10}	4.41×10^{-17}
240	1.68×10^{-22}	9.19×10^{-29}	5.12×10^{-9}	9.80×10^{-16}	3.04×10^{4}	2.49×10^{-4}	2.41×10^{-8}	9.53×10^{-15}
260	5.22×10^{-20}	1.25×10^{-25}	1.29×10^{-7}	1.13×10^{-13}	1.06×10^{5}	4.65×10^{-3}	6.65×10^{-7}	8.98×10^{-13}
280	7.03×10^{-18}	6.03×10^{-23}	1.99×10^{-6}	6.58×10^{-12}	3.05×10^{5}	5.73×10^{-2}	1.12×10^{-5}	4.40×10^{-11}
300	4.87×10^{-16}	1.28×10^{-20}	2.11×10^{-5}	2.21×10^{-10}	7.55×10^{5}	5.06×10^{-1}	1.29×10^{-4}	1.28×10^{-9}

Table S3. The imaginary frequencies (v_{im}, cm^{-1}) (Ref. 1) of the transition states (TSs) and the Wigner tunneling correction factor ($\Gamma(T)$) at different temperatures (220, 240, 260, 280 and 300 K) for hydration reactions of **GA** with **W** (a) uncatalyzed, (b) catalyzed by **W**, (c) **SA** and (d) **A** at M06-2X/6-311++G(3df,3pd) level of theory.

Temperatures	v_{im} (a)	$\Gamma(T)$ (a)	v_{im} (b)	$\Gamma(T)$ (b)	v_{im} (c)	$\Gamma(T)$ (c)	v_{im} (d)	$\Gamma(T)$ (d)
220	1368	4.34	827	2.22	277	1.14	558	1.56
240		3.81		2.02		1.12		1.48
260		3.39		1.87		1.10		1.40
280		3.06		1.75		1.08		1.34
300		2.80		1.66		1.07		1.30

Table S4. The rate constants of the forward and reverse reactions ($k_{1,cor}$ and $k_{-1,cor}$(s^{-1})) corrected by the tunneling effect factor $\Gamma(T)$ according to Wigner for the hydration reactions of **GA** with **W** (a) uncatalyzed, (b) catalyzed by **W**, (c) **SA** and (d) **A** at the different temperatures of 220, 240, 260, 280 and 300 K.

Temperatures	$k_{1,cor}$ (a)	$k_{-1,cor}$ (a)	$k_{1,cor}$ (b)	$k_{-1,cor}$(b)	$k_{1,cor}$ (c)	$k_{-1,cor}$ (c)	$k_{1,cor}$(d)	$k_{-1,cor}$(d)
220	8.16×10^{-25}	7.94×10^{-32}	2.44×10^{-10}	7.86×10^{-18}	7.81×10^{-3}	8.95×10^{-6}	1.05×10^{-9}	9.86×10^{-17}
240	6.40×10^{-22}	3.50×10^{-28}	1.04×10^{-8}	1.99×10^{-15}	3.39×10^{-4}	2.78×10^{-4}	4.91×10^{-8}	1.94×10^{-14}
260	1.77×10^{-19}	4.24×10^{-25}	2.42×10^{-7}	2.12×10^{-13}	1.16×10^{-5}	5.11×10^{-3}	1.25×10^{-6}	1.69×10^{-12}
280	2.15×10^{-17}	1.85×10^{-22}	3.49×10^{-6}	1.15×10^{-11}	3.31×10^{-5}	6.21×10^{-2}	1.98×10^{-5}	7.75×10^{-11}
300	1.36×10^{-15}	3.58×10^{-20}	3.50×10^{-5}	3.66×10^{-10}	8.11×10^{-5}	5.43×10^{-1}	2.15×10^{-4}	2.13×10^{-9}

Table S5. The evaporation rate coefficients (s^{-1}) of all studied clusters at varying temperatures ranging from 220 K to 300 K.

Clusters	300 K	280 K	260 K	240 K	220 K
$(SA)_2 \rightarrow SA+SA$	1.3E+03	1.5E+02	1.2E+01	0.6E+00	4.0E-02
$(SA)_1A_1 \rightarrow A+SA$	3.4E+04	5.0E+03	5.4E+02	4.1E+01	1.9E+00
$(SA)_2A_1 \rightarrow (SA)_1A_1+SA$	3.1E+00	1.3E-01	3.3E-03	4.5E-05	2.8E-07
$(SA)_2A_1 \rightarrow A+(SA)_2$	5.5E+01	2.8E+00	9.7E-02	1.9E-03	1.7E-05
$(GA)_1(SA)_1 \rightarrow GA+SA$	2.7E+05	3.6E+04	3.6E+03	2.4E+02	9.9E+00
$(GA)_1(SA)_2 \rightarrow (GA)_1(SA)_1+SA$	8.1E+04	8.0E+03	5.6E+02	2.6E+01	6.5E-01
$(GA)_1(SA)_2 \rightarrow (SA)_2+GA$	6.9E+06	8.0E+05	6.8E+04	4.0E+03	1.3E+02
$(GA)_1A_1 \rightarrow GA+A$	1.4E+08	3.3E+07	6.6E+06	9.6E+05	1.8E+06
$(GA)_1(SA)_1A_1 \rightarrow (GA)_1A_1+SA$	7.0E+01	5.3E+00	2.6E-01	8.1E-03	7.2E-06

Reaction					
$(GA)_1(SA)_1A_1 \rightarrow (GA)_1(SA)_1+A$	5.2E+04	7.1E+03	7.0E+02	4.7E+01	1.9E+00
$(GA)_1(SA)_1A_1 \rightarrow (SA)_1A_1+GA$	2.5E+05	3.2E+04	2.9E+03	1.7E+02	6.0E+00
$(GW)_1(SA)_1 \rightarrow GW+SA$	7.7E+05	9.6E+04	8.8E+03	5.3E+02	1.9E+01
$(GW)_1(SA)_2 \rightarrow (GW)_1(SA)_1+SA$	7.2E+04	7.3E+03	5.1E+02	2.3E+01	6.0E-01
$(GW)_1(SA)_2 \rightarrow (GW)_1+(SA)_2$	2.1E+07	2.3E+06	1.8E+05	9.7E+03	2.8E+02
$(GW)_1A_1 \rightarrow GW+A$	5.5E+08	1.4E+08	3.0E+07	4.7E+06	1.1E+05
$(GW)_1(SA)_1A_1 \rightarrow (GW)_1A_1+SA$	1.5E+02	8.4E+00	3.2E-01	6.8E-03	3.4E-04
$(GW)_1(SA)_1A_1 \rightarrow (GW)_1(SA)_1+A$	1.1E+05	1.3E+04	1.1E+03	6.2E+01	2.0E+00
$(GW)_1(SA)_1A_1 \rightarrow GW+(SA)_1A_1$	1.8E+06	1.9E+05	1.3E+04	6.0E+02	1.5E+01

Table S6. Cartesian coordinate of **SA**.

Atoms	X	Y	Z
S	0.000000	0.00000000	0.15432300
O	0.000000	1.24571500	0.82033500
O	0.000000	-1.24571500	0.82033500
O	1.223691	-0.04024200	-0.83614500
O	-1.223691	0.04024200	-0.83614500
H	-1.452033	-0.85852000	-1.10809700
H	1.452033	0.85852000	-1.10809700

Table S7. Cartesian coordinate of $(SA)_1W_1$.

Atoms	X	Y	Z
S	0.574277	-0.075955	0.121591
O	-0.215605	0.288808	1.248460
O	1.737700	-0.870444	0.247437
O	-0.338533	-0.732296	-0.941762
O	0.979121	1.291265	-0.552739
H	-1.289890	-0.469017	-0.773800
H	1.736148	1.150356	-1.135650

O	-2.661959	0.105985	-0.109758
H	-2.259274	0.361340	0.731812
H	-3.381199	-0.493949	0.099086

Table S8. Cartesian coordinate of $(SA)_1W_2$.

Atoms	X	Y	Z
S	0.986992	-0.150388	-0.099481
O	0.432583	1.170078	-0.640315
O	1.134685	0.126299	1.452466
O	-0.005244	-1.171702	-0.181044
O	2.277203	-0.349376	-0.644188
H	-0.562404	1.301754	-0.403772
H	1.971276	0.580502	1.615265
H	-2.423091	0.553179	-0.021326
O	-2.007743	1.446196	-0.076036
H	-2.204764	1.896542	0.747917
H	-1.846181	-1.395479	0.029141
O	-2.764155	-1.093281	0.112361
H	-3.265331	-1.555999	-0.561485

Table S9. Cartesian coordinate of $(SA)_1W_3$.

Atoms	X	Y	Z
O	-1.506990	-1.371735	-1.163177
H	-1.773950	-0.567008	-1.621186
H	-1.971831	-1.328300	-0.314030
S	1.244190	0.029228	0.161933
O	2.620912	0.184108	0.414141
O	1.056128	-1.232150	-0.708744
O	0.784181	1.192212	-0.765548

O	0.322056	-0.028098	1.266286
H	0.082261	-1.372103	-0.911487
H	-0.192657	1.341878	-0.695079
O	-1.876525	1.466547	-0.654087
H	-2.225041	1.049168	0.154071
H	-2.243910	2.351570	-0.702420
O	-2.325355	-0.349927	1.336061
H	-2.804143	-0.522403	2.148080
H	-1.373038	-0.308106	1.551677

Table S10. Cartesian coordinate of $(SA)_1W_4$.

Atoms	X	Y	Z
S	1.123487	-0.004287	-0.013165
O	0.739603	-1.272553	0.590085
O	0.706005	0.133641	-1.391936
O	2.705172	-0.008742	-0.115936
O	0.761365	1.128796	0.824541
H	3.083838	-0.065877	0.769689
H	-0.467606	2.096555	-0.086629
O	-1.312734	-1.687785	-1.555681
H	-0.980622	-2.425085	-1.032924
H	-0.510192	-1.161006	-1.743361
O	-2.367127	0.028387	-0.010740
H	-2.009490	-0.700950	-0.642459
H	-2.007591	-0.175284	0.931298
O	-1.303753	-0.538247	2.221235
H	-0.985665	0.265340	2.644566
H	-0.496223	-0.931638	1.828969
O	-1.265682	2.224447	-0.638203

Atoms	X	Y	Z
H	-0.927870	2.167923	-1.538213
H	-1.977167	0.935061	-0.307204

Table S11. Cartesian coordinate of (**SA**)₁**W**₅.

Atoms	X	Y	Z
S	-0.273434	-0.246988	-0.622495
O	-0.398343	1.167897	-0.272211
O	0.858168	-0.497366	-1.519686
O	-0.235248	-1.082549	0.570541
O	-1.500468	-0.644089	-1.461085
H	1.097808	2.037633	0.038707
O	-3.592423	-0.119444	-0.067986
H	-3.200360	0.217815	0.769273
H	-2.360318	-0.453730	-0.954804
H	-4.166899	0.571888	-0.402824
H	2.233097	3.046937	-0.317646
O	2.033085	2.275923	0.216811
H	2.774329	0.930368	-0.062445
H	2.850674	-0.646137	0.453583
O	2.973273	-0.024198	-0.342109
H	2.137529	-0.257546	-0.941678
H	-1.612224	-0.098600	2.178047
O	-2.087523	0.721596	2.004566
H	-1.477711	1.191145	1.416651
H	2.483859	-2.537246	1.475842
O	2.240301	-1.609699	1.501551
H	1.288589	-1.555293	1.264080

Table S12. Cartesian coordinate of **A**.

Atoms	X	Y	Z
N	0.000000	0.113488	0.000000
H	-0.939049	-0.264998	0.000000
H	0.469524	-0.264710	0.813353
H	0.469524	-0.264710	-0.813353

Table S13. Cartesian coordinate of A_1W_1.

Atoms	X	Y	Z
N	1.379382	0.022191	-0.000290
H	1.906343	0.877370	-0.125814
H	1.651266	-0.610741	-0.742711
H	1.681236	-0.392918	0.872774
O	-1.546280	-0.104761	-0.000013
H	-1.938012	0.768906	-0.000235
H	-0.586266	0.040132	-0.001883

Table S14. Cartesian coordinate of A_1W_2.

Atoms	X	Y	Z
N	1.592765	0.547711	-0.000357
H	2.123148	0.822936	0.816595
H	0.774022	1.149874	-0.055052
H	2.169493	0.731535	-0.811561
O	-0.261677	-1.561856	-0.096764
H	-0.230616	-2.187599	0.627884
H	0.546715	-1.012136	-0.023082
O	-1.377614	0.993459	0.076976
H	-2.180150	1.174600	-0.412842
H	-1.237645	0.033985	0.018858

Table S15. Cartesian coordinate of **W**.

Atoms	X	Y	Z
O	0.000000	0.000000	0.116638
H	0.000000	0.760974	-0.466554
H	0.000000	-0.760974	-0.466554

Table S16. Cartesian coordinate of **GA**.

Atoms	X	Y	Z
C	0.937401	-0.551457	0.000003
O	1.853227	0.206905	-0.000003
H	1.042330	-1.647548	0.000010
C	-0.527858	-0.103639	0.000002
O	-1.418093	-0.901561	-0.000003
O	-0.670546	1.215069	0.000001
H	-1.616295	1.414820	0.000001

Table S17. Cartesian coordinate of $(GA)_1W_1$.

Atoms	X	Y	Z
C	-1.773556	0.371946	0.002672
O	-2.503808	-0.566636	0.014299
H	-2.116451	1.418692	-0.002761
C	-0.245099	0.252841	-0.003052
O	0.428977	1.254323	0.001637
O	0.194631	-0.979595	-0.010335
H	1.181337	-0.959835	-0.011526
O	2.776772	-0.269251	-0.076082
H	3.465216	-0.341379	0.587477
H	2.409256	0.623067	-0.007067

Table S18. Cartesian coordinate of $(GA)_1W_2$.

Atoms	X	Y	Z
C	2.268885	-0.526623	0.012126
O	3.115796	0.308027	0.002204
H	2.473643	-1.609225	0.035909
C	0.766762	-0.209344	-0.003358
O	-0.016603	-1.133549	0.022714
O	0.489687	1.055294	-0.043154
H	-0.505520	1.222356	-0.046673
H	-1.849763	-1.302257	0.054742
O	-2.797083	-1.084863	0.077183
H	-3.208855	-1.588488	-0.626722
H	-2.514343	0.616204	-0.033310
H	-2.424538	2.017445	0.644630
O	-2.064862	1.487562	-0.069096

Table S19. Cartesian coordinate of **GW**.

Atoms	X	Y	Z
C	0.753152	0.152247	0.021681
O	1.046470	1.177502	-0.520231
O	1.618142	-0.797417	0.364226
H	2.497574	-0.522761	0.071931
C	-0.690334	-0.211143	0.373777
H	-0.738952	-0.658178	1.368510
O	-1.475214	0.922130	0.387706
O	-1.065270	-1.131827	-0.612958
H	-1.990135	-1.354502	-0.475747
H	-1.138422	1.525711	-0.287391

Table S20. Cartesian coordinate of $(GW)_1W_1$.

Atoms	X	Y	Z
C	-0.100803	0.021841	-0.164147
O	-0.553776	1.035422	0.312599
O	-0.804089	-1.006897	-0.574167
H	-1.758092	-0.828473	-0.399892
C	1.408717	-0.173047	-0.318411
H	1.631543	-0.653977	-1.272459
O	2.055465	1.045564	-0.302647
O	1.762141	-0.996893	0.758689
H	2.714931	-1.120693	0.737529
H	1.566169	1.630128	0.290656
O	-3.169601	0.079585	0.093383
H	-3.737118	-0.159145	0.828632
H	-2.586034	0.785154	0.408025

Table S21. Cartesian coordinate of $(GW)_1W_2$.

Atoms	X	Y	Z
C	0.410404	-0.136436	-0.199427
O	-0.171985	0.900405	0.038681
O	-0.136289	-1.297203	-0.403205
H	-1.137525	-1.267908	-0.301359
C	1.940395	-0.161849	-0.260948
H	2.274096	-0.813024	-1.070377
O	2.438453	1.101343	-0.509417
O	2.327231	-0.666352	0.988055
H	3.287488	-0.658894	1.025762
H	1.861566	1.734036	-0.062628
O	-2.724486	-1.242450	-0.154557

H	-3.087545	-1.768685	0.560291
H	-2.978371	-0.311887	0.023601
O	-2.881731	1.382632	0.359638
H	-3.220931	2.053596	-0.234720
H	-1.913120	1.395476	0.268122

Table S22. Cartesian coordinate of $(GA)_1A_1$.

Atoms	X	Y	Z
C	-1.830481	0.299795	0.000001
O	-2.492274	-0.689611	-0.000002
H	-2.253413	1.317928	0.000015
C	-0.296509	0.300354	0.000000
O	0.289417	1.355794	-0.000002
O	0.240463	-0.889003	0.000001
H	1.246976	-0.789390	0.000004
N	2.854420	-0.291888	0.000001
H	3.412106	-0.504680	0.817992
H	2.662385	0.705742	-0.000017
H	3.412097	-0.504710	-0.817987

Table S23. Cartesian coordinate of $(GA)_1A_2$.

Atoms	X	Y	Z
C	-2.2764340	-0.527586	0.002366
O	-3.1274000	0.303790	-0.012335
H	-2.4803850	-1.611003	0.015261
C	-0.7735990	-0.208338	0.004534
O	0.0037900	-1.140096	0.012915
O	-0.4928000	1.051646	-0.003247
H	0.5298590	1.234946	-0.002381

O	2.7983530	-1.214863	0.041521
H	1.8342740	-1.328790	0.031431
H	3.1679570	-2.001174	-0.360567
N	2.0714330	1.592109	-0.004088
H	2.6028090	0.725826	-0.099313
H	2.3622380	2.038516	0.857677
H	2.3278720	2.208643	-0.765729

Table S24. Cartesian coordinate of $(GA)_1(SA)_1$.

Atoms	X	Y	Z
C	3.499741	0.424197	0.083955
O	4.294040	-0.458070	0.116784
H	3.754563	1.493175	0.149405
C	1.991415	0.177965	-0.056311
O	1.248044	1.141253	-0.078066
O	1.653496	-1.066657	-0.137542
H	0.669790	-1.162525	-0.210016
S	-1.939394	-0.105572	-0.081688
O	-3.232189	-0.167175	-0.643675
O	-0.995860	-1.158964	-0.300894
O	-2.063102	-0.018147	1.485725
O	-1.300394	1.236074	-0.468754
H	-2.870017	0.457366	1.724169
H	-0.303245	1.221649	-0.311028

Table S25. Cartesian coordinate of $(GA)_1(SA)_1W_1$.

Atoms	X	Y	Z
C	3.894519	-0.665606	-0.001186
O	4.726787	-0.021225	-0.551770

H	4.081624	-1.635658	0.484878
C	2.430370	-0.218447	0.104854
O	1.649316	-0.937850	0.698450
O	2.169503	0.910831	-0.466263
H	1.209337	1.146480	-0.368161
S	-1.425778	0.458594	0.184391
O	-2.678302	0.910966	0.680489
O	-0.403562	1.416626	-0.118629
O	-1.644215	-0.363683	-1.107733
O	-0.870004	-0.560913	1.197376
H	-2.557474	-0.774837	-1.084633
H	0.105096	-0.733525	1.024797
O	-4.120178	-1.071816	-0.736284
H	-4.217493	-0.395705	-0.051767
H	-4.392739	-1.903436	-0.342459

Table S26. Cartesian coordinate of $(GA)_1(SA)_1W_2$.

Atoms	X	Y	Z
C	-4.247518	0.730018	0.244449
O	-5.117293	0.274339	-0.424124
H	-4.379090	1.569726	0.944667
C	-2.807760	0.199608	0.215269
O	-1.978900	0.746365	0.918505
O	-2.618705	-0.801804	-0.578111
H	-1.670252	-1.103978	-0.555456
S	0.976763	-0.644549	-0.023150
O	2.238194	-1.227299	0.289858
O	-0.091380	-1.521985	-0.407413
O	1.113648	0.393395	-1.138318

O	0.543488	0.169224	1.216801
H	1.922419	1.022652	-0.981282
H	-0.425179	0.419046	1.139136
O	3.109962	1.855665	-0.728937
H	3.808451	1.293991	-0.314967
H	2.966775	2.602993	-0.144029
O	4.684796	0.092463	0.468609
H	3.976765	-0.567582	0.530583
H	5.433090	-0.344733	0.058480

Table S27. Cartesian coordinate of $(GA)_1(SA)_1W_3$.

Atoms	X	Y	Z
C	4.074237	-0.978923	0.448564
O	4.496255	-1.886128	-0.192969
H	4.537715	-0.612732	1.378605
C	2.819657	-0.183773	0.061965
O	2.491184	0.749465	0.761479
O	2.231037	-0.607042	-1.011486
H	1.401559	-0.095109	-1.197017
S	-1.162925	0.427994	-0.636186
O	-2.352381	-0.044437	-1.265150
O	-0.026603	0.713624	-1.468274
O	-0.661751	-0.574360	0.415129
O	-1.540741	1.680268	0.163691
H	-1.425270	-0.894970	1.034063
H	-0.688473	2.144411	0.513466
O	-2.574910	-1.349238	1.850037
H	-3.345529	-1.467726	1.244591
H	-2.849962	-0.739741	2.538567

O	-4.428403	-1.437043	-0.045558
H	-3.871634	-0.944369	-0.669448
H	-4.688437	-2.245203	-0.491180
O	0.612045	2.699165	0.973566
H	0.916220	3.431313	0.431927
H	1.291388	1.998213	0.888509

Table S28. Cartesian coordinate of $(GA)_1(SA)_1A_1$.

Atoms	X	Y	Z
C	3.917446	-0.642819	0.066145
O	4.721411	-0.132275	-0.644569
H	4.138542	-1.476618	0.750983
C	2.449210	-0.200650	0.122350
O	1.700128	-0.791243	0.876719
O	2.151479	0.781471	-0.661821
H	1.186546	1.023854	-0.578556
S	-1.411187	0.482440	0.162107
O	-2.636515	1.057748	0.596247
O	-0.382063	1.350881	-0.343252
O	-1.681086	-0.576440	-0.911039
O	-0.830995	-0.311797	1.356406
H	-2.682304	-0.905013	-0.852285
H	0.133338	-0.523102	1.200108
N	-4.168810	-1.177087	-0.662384
H	-4.722428	-1.102089	-1.507232
H	-4.426338	-0.412513	-0.044044
H	-4.405497	-2.049887	-0.206483

Table S29. Cartesian coordinate of $(GA)_1(SA)_1A_1W_1$.

Atoms	X	Y	Z
C	4.135356	0.646155	0.481848
O	4.994569	-0.170824	0.570596
H	4.275517	1.713478	0.717437
C	2.705553	0.322544	0.027703
O	1.900118	1.233536	-0.006113
O	2.504492	-0.914182	-0.277168
H	1.552685	-1.067842	-0.574642
S	-0.995149	-0.477574	-0.409733
O	-2.308913	-0.643894	-0.988868
O	0.066489	-1.213453	-1.063167
O	-1.009513	-0.707800	1.041918
O	-0.684820	1.051813	-0.606957
H	-2.457737	-0.617653	1.489366
H	0.272157	1.208573	-0.398003
N	-3.535460	-0.488605	1.553882
H	-3.958015	-1.241250	1.016140
H	-3.738561	0.409736	1.060211
H	-3.881795	-0.489878	2.506486
O	-3.719113	1.611883	-0.202439
H	-3.270131	1.002193	-0.813199
H	-3.115441	2.355239	-0.124956

Table S30. Cartesian coordinate of $(GA)_1(SA)_1A_1W_3$.

Atoms	X	Y	Z
C	-3.174897	-1.452543	-0.330010
O	-2.661412	-2.493345	-0.622441
H	-4.215298	-1.206681	-0.586363
C	-2.392144	-0.320415	0.342952

O	-2.765351	0.815554	0.170466
O	-1.360941	-0.735958	1.002081
H	-0.666954	0.015446	1.184995
S	1.124563	1.094851	-0.091864
O	2.515633	0.718402	-0.111814
O	0.509575	0.880103	1.239067
O	0.317304	0.442892	-1.119107
O	1.092516	2.617303	-0.348918
H	0.306967	-1.269494	-0.941392
H	0.141641	2.939417	-0.284202
N	0.354543	-2.253281	-0.590124
H	0.781906	-2.180871	0.364850
H	0.986049	-2.787824	-1.179925
H	-0.591102	-2.636943	-0.540483
O	1.756961	-1.730067	1.710539
H	2.603498	-1.716329	1.246093
H	1.558404	-0.801151	1.895787
O	-1.418214	3.246898	-0.164032
H	-1.812458	3.504043	-1.000409
H	-1.873344	2.425877	0.091071
O	3.108493	-1.833140	-0.845148
H	3.959359	-1.953298	-1.269538
H	2.992271	-0.868234	-0.742989

Table S31. Cartesian coordinate of $(GA)_1(SA)_1A_1W_4$.

Atoms	X	Y	Z
C	3.077324	-1.412009	0.108712
O	2.573392	-2.400892	0.556618
H	4.114392	-1.115856	0.317606

C	2.311367	-0.434323	-0.788312
O	2.822613	0.588735	-1.156919
O	1.101321	-0.854636	-1.037923
H	0.460148	-0.119235	-1.313198
S	-1.350024	1.125143	-0.022640
O	-2.773635	0.939351	0.049593
O	-0.790756	0.782206	-1.340510
O	-0.636929	0.391761	1.038943
O	-1.077293	2.625936	0.204709
H	-0.530634	-1.346885	0.926914
H	-0.082844	2.794160	0.108682
N	-0.480825	-2.335379	0.605753
H	-0.956642	-2.318270	-0.329138
H	-1.005817	-2.926133	1.241818
H	0.503130	-2.603265	0.514993
O	-2.011985	-1.863067	-1.610283
H	-2.806121	-1.780672	-1.064619
H	-1.788526	-0.955633	-1.861581
O	1.487529	2.816228	0.005138
H	1.869965	2.246363	0.692055
H	1.823141	2.433076	-0.814903
O	-3.250306	-1.634222	0.939126
H	-4.095686	-1.782543	1.366106
H	-3.186785	-0.670224	0.802621
O	1.958843	0.645975	1.761237
H	2.100232	0.698416	2.708257
H	0.993709	0.571056	1.626117

Table S32. Cartesian coordinate of $(GA)_1A_2$.

Atoms	X	Y	Z
H	-0.412898	1.279890	0.005150
N	-1.954746	1.668330	-0.029875
H	-2.211614	2.156758	-0.879561
H	-2.232134	2.255488	0.747796
H	-2.501960	0.801717	0.013954
N	-3.064692	-1.161282	0.067091
H	-3.542597	-1.602327	-0.708898
H	-3.423940	-1.585940	0.913065
H	-2.079154	-1.404296	-0.001634
C	2.304774	-0.603274	-0.005945
O	3.196208	0.182480	0.064298
H	2.457511	-1.694139	-0.060791
C	0.818889	-0.213921	-0.030466
O	-0.003355	-1.099835	-0.101845
O	0.599755	1.060690	0.028656

Table S33. Cartesian coordinate of $(GA)_1A_2W_1$.

Atoms	X	Y	Z
H	-0.106502	1.405760	-0.126554
N	-1.530015	1.752068	-0.111556
H	-1.988269	1.403620	-0.948962
H	-1.734410	2.737784	-0.005629
H	-1.941556	1.230712	0.669362
N	-2.377110	-0.553341	1.610520
H	-2.814324	-0.845714	2.474919
H	-1.475322	-1.014578	1.547324
H	-2.927347	-0.915887	0.838455
C	2.563193	-0.611511	0.071342

O	3.487468	0.128678	0.188648
H	2.660526	-1.710080	0.059187
C	1.107135	-0.139781	-0.078810
O	0.247446	-1.002475	-0.177280
O	0.941133	1.129470	-0.084012
O	-2.257148	-0.747698	-1.401010
H	-1.375038	-0.894856	-1.018497
H	-2.321040	-1.343902	-2.148300

Table S34. Cartesian coordinate of $(GA)_1(SA)_2$.

Atoms	X	Y	Z
C	-4.854272	-1.352555	0.038540
O	-5.901396	-0.854907	0.292700
H	-4.697300	-2.429376	-0.125371
C	-3.564360	-0.530539	-0.094993
O	-2.529495	-1.118001	-0.359996
O	-3.712169	0.737862	0.093465
H	-2.855691	1.221955	-0.002750
S	-0.069693	1.178428	-0.076187
O	1.121071	1.758953	-0.598911
O	-1.303871	1.879646	-0.217977
O	0.090685	0.867153	1.421753
O	-0.193328	-0.217934	-0.740876
H	0.943911	0.366823	1.548723
H	-1.129274	-0.607249	-0.591836
S	3.238374	-0.673195	0.139466
O	2.307834	-0.486391	1.221733
O	4.406303	-1.425395	0.338897
O	3.658443	0.719548	-0.397570

O	2.451941	-1.308290	-1.048875
H	2.870020	1.291448	-0.504056
H	1.513075	-1.046722	-1.033200

Table S35. Cartesian coordinate of $(GA)_1(SA)_2W_1$.

Atoms	X	Y	Z
C	5.444169	0.417658	0.955211
O	6.371745	-0.289636	0.735193
H	5.472713	1.297238	1.615973
C	4.062144	0.184202	0.328559
O	3.162411	0.956746	0.607401
O	3.991814	-0.840340	-0.454932
H	3.081846	-0.948470	-0.825062
S	0.341740	-0.332651	-0.760639
O	-0.816983	-0.095546	-1.577159
O	1.471961	-0.961541	-1.365798
O	-0.041635	-1.161527	0.461682
O	0.749881	1.049152	-0.212343
H	-0.920363	-0.821578	0.863924
H	1.708908	1.030132	0.129822
S	-3.489600	-0.289920	0.593502
O	-2.199581	-0.140128	1.245163
O	-4.534906	-0.930799	1.279219
O	-3.247219	-1.068164	-0.733381
O	-3.946197	1.104821	0.157250
H	-2.414170	-0.785394	-1.167194
H	-3.165319	1.677330	-0.155394
O	-1.922590	2.434254	-0.669810
H	-1.465447	1.864792	-1.302839

Atoms	X	Y	Z
H	-1.279897	2.577589	0.032464

Table S36. Cartesian coordinate of $(GA)_1(SA)_2W_2$.

Atoms	X	Y	Z
C	5.4932720	-0.050475	-1.190379
O	6.5186910	0.041457	-0.598877
H	5.4068420	-0.074961	-2.287364
C	4.1350740	-0.146990	-0.481477
O	3.1311360	-0.228306	-1.166352
O	4.1979650	-0.129128	0.808418
H	3.2960640	-0.187496	1.215455
S	0.5563540	0.069944	0.995156
O	-0.7113110	-0.407502	1.470199
O	1.7109010	-0.317059	1.748215
O	0.5708120	1.575303	0.859158
O	0.6825660	-0.470960	-0.450792
H	-0.1655480	1.968778	0.187821
H	1.6405420	-0.381596	-0.772218
S	-3.6379730	0.036246	-0.390801
O	-2.4725080	0.242964	-1.225249
O	-4.8431160	0.694144	-0.703006
O	-3.2441930	0.468915	1.055266
O	-3.8810460	-1.474049	-0.300433
H	-2.3329540	0.170877	1.275300
H	-2.9939220	-1.973143	-0.346567
O	-1.0833350	2.440020	-0.729100
H	-1.6400240	1.686959	-1.039798
H	-1.6814670	3.119760	-0.406455
O	-1.5472430	-2.505861	-0.397696

Atoms	X	Y	Z
H	-1.1645850	-2.440865	0.484752
H	-1.0636860	-1.842066	-0.907483

Table S37. Cartesian coordinate of (**GA**)$_1$(**SA**)$_2$**W**$_3$.

Atoms	X	Y	Z
C	5.576830	0.446340	-1.141497
O	6.581122	0.606250	-0.527597
H	5.497121	0.543382	-2.235418
C	4.242302	0.078537	-0.478375
O	3.268135	-0.067869	-1.194012
O	4.291315	-0.039584	0.805767
H	3.398072	-0.279802	1.182011
S	0.695173	-0.303453	1.000734
O	-0.482292	-1.054752	1.427416
O	1.905644	-0.706680	1.668229
O	0.472723	1.140194	1.060010
O	0.834327	-0.679420	-0.512955
H	-0.363994	1.821520	0.108053
H	1.762917	-0.459548	-0.824331
S	-3.223783	-0.261356	-0.425818
O	-2.109307	-0.020780	-1.322229
O	-4.400771	0.514763	-0.613504
O	-2.748911	0.013282	1.015816
O	-3.561605	-1.744116	-0.488304
H	-1.842367	-0.406897	1.220953
H	-2.681742	-2.289393	-0.567262
O	-0.999477	2.204969	-0.627007
H	-1.341151	1.387333	-1.092482
H	-1.834647	2.612177	-0.209493

O	-1.300715	-2.846904	-0.617065
H	-0.894374	-2.659400	0.242520
H	-0.800170	-2.284312	-1.222592
O	-3.262660	3.000523	0.268399
H	-3.368611	3.016086	1.223701
H	-3.888314	2.327519	-0.048809

Table S38. Cartesian coordinate of $(GA)_1(SA)_2W_4$.

Atoms	X	Y	Z
C	-5.816144	0.482879	0.932317
O	-6.749814	0.783691	0.262263
H	-5.830991	0.440126	2.032500
C	-4.450336	0.110708	0.338677
O	-3.552204	-0.183536	1.107962
O	-4.392187	0.150030	-0.948730
H	-3.483117	-0.103247	-1.280489
S	-0.830936	-0.247141	-0.886667
O	0.381202	-0.941147	-1.308091
O	-1.988122	-0.568685	-1.683361
O	-0.616072	1.184459	-0.744440
O	-1.103005	-0.810943	0.558660
H	0.316886	1.834560	0.271418
H	-2.050902	-0.587371	0.815492
S	3.323326	0.005651	0.116650
O	2.304829	-0.030071	1.188413
O	4.376512	0.943720	0.355077
O	2.572967	0.581077	-1.138401
O	3.757397	-1.346672	-0.207635
H	1.754982	0.057050	-1.321672

Atoms	X	Y	Z
H	2.710887	-2.368629	-0.338401
O	0.988003	2.131120	0.978203
H	1.479251	1.272360	1.218947
H	1.721499	2.721188	0.563099
O	1.858119	-2.964650	-0.348498
H	1.228408	-2.484318	-0.929521
H	1.450241	-2.825698	0.616109
O	3.005906	3.367664	0.076636
H	2.996905	3.585635	-0.859432
H	3.683713	2.671502	0.174101
O	0.930056	-2.343997	1.865405
H	0.063699	-1.970677	1.644226
H	1.490474	-1.556643	1.980245

Table S39. Cartesian coordinate of $(GA)_1(SA)_2W_5$.

Atoms	X	Y	Z
C	6.056714	-0.589161	0.783407
O	6.963551	-0.714271	0.026177
H	6.134627	-0.733084	1.872268
C	4.641794	-0.202745	0.331409
O	3.778269	-0.088487	1.182760
O	4.510032	-0.033694	-0.940629
H	3.572870	0.222113	-1.178357
S	0.939022	0.188752	-0.637897
O	-0.300135	0.928060	-0.865588
O	2.043029	0.671017	-1.433998
O	0.751271	-1.248540	-0.733124
O	1.276346	0.511800	0.861310
H	-0.234999	-2.091432	0.094750

H	2.239937	0.286736	1.039865
S	-3.328812	-0.365751	0.162010
O	-2.361598	-0.531567	1.271085
O	-4.298536	-1.419029	0.095124
O	-2.477643	-0.546922	-1.146102
O	-3.880212	0.976543	0.157585
H	-1.666349	0.021231	-1.115018
H	-3.060502	2.234497	0.400761
O	-0.940422	-2.540458	0.669144
H	-1.489614	-1.767172	1.051042
H	-1.609933	-3.054501	0.078148
O	-2.417313	2.987860	0.637304
H	-1.915133	3.268606	-0.191521
H	-1.746558	2.544224	1.307161
O	-2.801654	-3.617676	-0.657779
H	-2.708321	-3.601961	-1.614004
H	-3.515716	-2.981230	-0.453062
O	-0.948446	3.523480	-1.394780
H	-1.244298	3.798628	-2.264601
H	-0.513574	2.659592	-1.489018
O	-0.976861	1.695049	2.199826
H	-1.459025	0.853365	2.108338
H	-0.095239	1.498487	1.852031

Table S40. Cartesian coordinate of $(GA)_1(SA)_2W_6$.

Atoms	X	Y	Z
C	-6.054094	-0.356575	-0.881206
O	-6.980782	-0.471460	-0.146843
H	-6.106584	-0.496658	-1.972055

C	-4.645706	0.008605	-0.392496
O	-3.758448	0.110681	-1.220660
O	-4.543337	0.174063	0.882896
H	-3.608207	0.413749	1.142803
S	-0.946651	0.360502	0.663677
O	0.272706	1.129296	0.917475
O	-2.074882	0.833046	1.432013
O	-0.717936	-1.069206	0.769224
O	-1.252575	0.663059	-0.844334
H	-0.232051	-2.079011	-0.767871
H	-2.218871	0.461376	-1.036188
S	3.164967	-0.337669	-0.428155
O	2.103820	-0.300785	-1.429009
O	3.895619	-1.586386	-0.400986
O	2.436510	-0.297294	0.968739
O	4.023798	0.832329	-0.490697
H	1.610534	0.262174	0.920785
H	3.319631	2.180185	-0.467003
O	0.374607	-2.483432	-1.410962
H	0.875814	-1.721279	-1.746609
H	1.411548	-3.144742	-0.613117
O	2.714656	3.003109	-0.515159
H	2.332133	3.210026	0.393737
H	1.929974	2.732903	-1.153606
O	2.170855	-3.444430	0.040680
H	1.811998	-3.199003	0.966329
H	2.943611	-2.815268	-0.142192
O	1.484425	3.441738	1.696741
H	1.867491	3.501908	2.573947

H	0.854148	2.703068	1.700826
O	0.963536	2.118448	-2.048780
H	1.322121	1.211357	-2.073223
H	0.085246	2.002558	-1.662514
O	1.174795	-2.590662	2.229481
H	1.805729	-1.901697	2.467056
H	0.402550	-2.096083	1.904205

Table S41. Cartesian coordinate of $(GA)_1(SA)_2W_7$.

Atoms	X	Y	Z
C	-6.166851	-0.191895	-0.934446
O	-7.119785	-0.149262	-0.226139
H	-6.204463	-0.422044	-2.010546
C	-4.741670	0.074498	-0.430691
O	-3.829041	0.017176	-1.235415
O	-4.653651	0.338235	0.828822
H	-3.703793	0.502970	1.098567
S	-1.037760	0.204021	0.701466
O	0.211461	0.924792	0.943221
O	-2.153464	0.795358	1.407703
O	-0.902406	-1.225541	0.897091
O	-1.300321	0.425895	-0.832300
H	-0.597277	-2.300550	-0.697170
H	-2.273708	0.272061	-1.031449
S	3.037266	-0.764988	-0.426424
O	1.898627	-0.676872	-1.337842
O	3.560608	-2.113447	-0.299890
O	2.452335	-0.438930	1.006022
O	4.055463	0.216793	-0.702907

H	1.620502	0.101358	0.936497
H	4.255593	1.753026	-0.088810
O	-0.010661	-2.719507	-1.346358
H	0.548632	-1.980893	-1.641988
H	0.983600	-3.479622	-0.538742
O	1.972881	3.529132	-0.563869
H	1.386739	3.642881	0.247445
H	1.541162	2.796816	-1.187519
O	1.730373	-3.819960	0.096807
H	1.448801	-3.493583	1.025277
H	2.540009	-3.234893	-0.117262
O	0.326617	3.616153	1.401069
H	0.477973	3.957018	2.284360
H	0.120214	2.668818	1.482023
O	0.950446	1.787025	-2.003410
H	1.404733	0.927123	-1.889522
H	0.044151	1.590967	-1.727963
O	1.065171	-2.681947	2.272520
H	1.758538	-2.009880	2.304842
H	0.273600	-2.184193	2.004860
O	4.231930	2.703487	0.169872
H	2.914894	3.236258	-0.277881
H	5.026478	3.107572	-0.184840

Table S42. Cartesian coordinate of $(GW)_1A_1$.

Atoms	X	Y	Z
C	0.065134	0.077338	0.1451150
O	0.449325	1.105055	-0.3612940
O	0.827708	-0.900381	0.5618290

Atoms	X	Y	Z
H	1.789455	-0.673973	0.3582680
C	-1.430931	-0.188863	0.3346450
H	-1.615803	-0.638909	1.3118620
O	-2.138632	0.995398	0.2732230
O	-1.766729	-1.077804	-0.6974430
H	-2.717843	-1.211872	-0.6703750
H	-1.650346	1.589747	-0.3122220
N	3.264842	-0.001907	-0.1359680
H	2.862377	0.865724	-0.4789930
H	3.738872	-0.453503	-0.9084890
H	3.960802	0.227143	0.5626360

Table S43. Cartesian coordinate of $(GW)_1A_1W_1$.

Atoms	X	Y	Z
C	0.416772	-0.162910	-0.202417
O	-0.155125	0.898308	-0.054405
O	-0.137428	-1.327361	-0.318916
H	-1.167377	-1.290429	-0.230664
C	1.948327	-0.198496	-0.242124
H	2.291987	-0.914410	-0.990444
O	2.454541	1.040587	-0.582640
O	2.321524	-0.601277	1.048833
H	3.280593	-0.568944	1.100010
H	1.848316	1.704667	-0.228775
N	-2.758548	-1.318474	-0.082650
H	-3.071114	-0.378420	0.163482
H	-3.066771	-1.955819	0.641767
H	-3.227380	-1.584698	-0.940251
O	-2.847421	1.567420	0.249522

	H	-2.970101	2.310856	0.840191
	H	-1.887639	1.453540	0.151332

Table S44. Cartesian coordinate of $(GW)_1(SA)_1$.

Atoms	X	Y	Z
C	1.903852	0.701398	-0.184520
O	0.999596	1.274481	-0.729725
O	2.894162	1.311830	0.444767
H	2.738286	2.265983	0.421979
C	2.062464	-0.821089	-0.098219
H	3.105514	-1.072577	-0.292851
O	1.759815	-1.287408	1.158790
O	1.227675	-1.359361	-1.096843
H	1.281168	-2.318955	-1.032538
H	0.846992	-1.026135	1.372128
S	-1.807924	0.015139	0.171762
O	-0.807682	-0.251725	1.165125
O	-3.165406	-0.240044	0.439441
O	-1.410124	-0.740690	-1.125927
O	-1.702439	1.515663	-0.241775
H	-0.432605	-0.873868	-1.167808
H	-0.775231	1.719507	-0.463486

Table S45. Cartesian coordinate of $(GW)_1(SA)_1W_1$.

Atoms	X	Y	Z
C	1.492559	-0.566742	0.463748
O	0.877115	-1.181547	-0.381900
O	1.006381	-0.062878	1.556938
H	0.003937	-0.077698	1.528915

C	2.969177	-0.240681	0.237126
H	3.534408	-0.300311	1.166620
O	3.538147	-1.091361	-0.673862
O	2.923558	1.098639	-0.225961
H	3.799067	1.337993	-0.544608
H	2.860217	-1.351249	-1.311981
S	-2.251789	-0.115600	-0.012143
O	-1.537771	0.210520	1.205554
O	-3.658284	-0.125356	0.007974
O	-1.780503	-1.513584	-0.488227
O	-1.748614	0.836353	-1.114850
H	-0.793676	-1.541690	-0.486429
H	-0.916336	1.336972	-0.843718
H	1.226198	1.938783	-0.452969
H	0.190292	2.389522	0.593139
O	0.299233	2.199441	-0.343157

Table S46. Cartesian coordinate of $(GW)_1(SA)_1W_2$.

Atoms	X	Y	Z
C	-2.363907	-0.201274	0.186703
O	-1.555112	0.600101	0.619529
O	-2.106808	-1.407472	-0.209880
H	-1.138097	-1.617685	-0.138951
C	-3.835457	0.195812	0.054052
H	-4.471443	-0.660233	0.282820
O	-4.157171	1.196787	0.946908
O	-3.958232	0.587549	-1.282999
H	-4.869135	0.853043	-1.436738
H	-3.425496	1.825962	0.968047

S	1.468184	-0.831029	0.059309
O	0.484636	-1.875235	0.066577
O	2.792313	-1.144199	0.484131
O	0.986023	0.329336	0.962810
O	1.471036	-0.242944	-1.352877
H	-0.006715	0.468521	0.845621
H	2.206460	0.477690	-1.459827
H	3.639001	1.561584	-0.570564
H	3.990255	1.351775	-2.080286
O	3.259810	1.521348	-1.481262
O	4.086052	1.298603	1.045338
H	3.794474	0.376782	1.118226
H	3.565561	1.780809	1.691976

Table S47. Cartesian coordinate of $(GW)_1(SA)_1W_3$.

Atoms	X	Y	Z
C	-2.225667	-1.446542	-0.420048
O	-2.096585	-2.499899	0.492785
H	-3.191523	-1.467009	-0.927531
C	-2.156773	-0.145775	0.399125
O	-2.398630	0.916753	-0.106431
O	-1.804924	-0.254033	1.668856
H	-1.575704	-1.182730	1.846696
O	-1.249272	-1.459171	-1.397920
H	-1.835130	-3.294126	0.017356
H	-0.385072	-1.386866	-0.939113
S	2.101147	-0.516820	0.074095
O	0.714103	-0.886371	0.297420
O	3.096613	-1.509797	0.189103

O	2.430782	0.629374	1.042729
O	2.195552	0.103908	-1.332512
H	1.599513	1.161173	1.295145
H	1.334061	0.563860	-1.611496
O	-0.007655	1.163422	-2.077937
H	-0.717249	0.508860	-2.038968
H	-0.326917	1.943811	-1.600427
O	0.313752	1.877386	1.698999
H	-0.051988	2.488338	1.040488
H	-0.370808	1.214091	1.852828
O	-1.029103	3.222872	-0.380241
H	-1.831936	2.705175	-0.217285
H	-1.288021	4.132879	-0.536476

Table S48. Cartesian coordinate of $(GW)_1(SA)_1A_1$.

Atoms	X	Y	Z
C	1.494616	-0.535948	0.461054
O	0.905402	-1.253696	-0.319672
O	0.975115	0.090826	1.472303
H	-0.035131	0.029342	1.452954
C	2.977661	-0.231696	0.246460
H	3.517989	-0.235101	1.193384
O	3.561189	-1.153131	-0.586785
O	2.960988	1.069198	-0.308592
H	3.851783	1.271576	-0.609225
H	2.887306	-1.473002	-1.201504
S	-2.227118	-0.159579	-0.027040
O	-1.564742	0.181988	1.223185
O	-3.636618	-0.147496	-0.042968

Atoms	X	Y	Z
O	-1.772966	-1.589332	-0.431679
O	-1.641488	0.727298	-1.118262
H	-0.788319	-1.623396	-0.430840
H	-0.875212	1.402839	-0.770365
N	0.125086	2.364446	-0.296403
H	-0.010220	3.266256	-0.739265
H	1.093637	2.081655	-0.435418
H	-0.012236	2.482610	0.702415

Table S49. Cartesian coordinate of $(GW)_1(SA)_1A_1W_1$.

Atoms	X	Y	Z
C	-1.604107	-0.449216	-0.636632
O	-1.249343	-1.574872	-0.368255
O	-0.880916	0.492561	-1.161642
H	0.117160	0.226703	-1.208701
C	-3.021594	0.016161	-0.296140
H	-3.505126	0.454755	-1.170579
O	-3.791655	-1.020515	0.163621
O	-2.829459	1.019080	0.693029
H	-3.684340	1.183890	1.101689
H	-3.199299	-1.718762	0.475401
S	1.927461	-0.716236	0.209122
O	1.570486	0.010494	-1.039836
O	3.321597	-0.756936	0.461057
O	1.468572	-2.195821	-0.030274
O	1.090222	-0.216092	1.304812
H	0.501852	-2.197229	-0.174757
H	0.379427	1.139643	1.238130
N	-0.096348	2.097679	1.110694

Atoms	X	Y	Z
H	-0.058996	2.624414	1.976734
H	-1.068672	1.944878	0.826394
H	0.444765	2.579410	0.370137
O	1.703342	2.754402	-0.892229
H	2.539777	3.220686	-0.927632
H	1.899949	1.817539	-1.073256

Table S50. Cartesian coordinate of $(GW)_1(SA)_1A_1W_2$.

Atoms	X	Y	Z
C	2.037073	-0.331718	0.553558
O	1.855291	-1.469000	0.183091
O	1.217000	0.401312	1.246803
H	0.299282	-0.056802	1.333466
C	3.313069	0.419190	0.167945
H	3.814000	0.804847	1.058074
O	4.183569	-0.394392	-0.512133
O	2.859787	1.503305	-0.629018
H	3.628942	1.861403	-1.081691
H	3.682408	-1.144529	-0.860491
S	-1.397625	-1.124758	-0.101480
O	-1.089688	-0.575554	1.234977
O	-2.799681	-1.320339	-0.315681
O	-0.758297	-2.555033	-0.134025
O	-0.720847	-0.352638	-1.137151
H	0.206331	-2.448132	-0.021623
H	-0.274224	1.189710	-0.989448
N	-0.050784	2.177167	-0.689722
H	-0.236683	2.828072	-1.444942
H	0.933803	2.210923	-0.415982

Atoms	X	Y	Z
H	-0.706734	2.349873	0.120485
O	-1.972676	2.178803	1.198368
H	-1.798362	1.315612	1.598870
H	-2.738260	1.999696	0.618664
O	-3.763474	1.287478	-0.691362
H	-4.719595	1.353849	-0.678100
H	-3.562145	0.335074	-0.665502

Table S51. Cartesian coordinate of $(GW)_1(SA)_1A_1W_3$.

Atoms	X	Y	Z
C	-2.124681	0.177631	0.499189
O	-2.150828	1.322678	0.106635
O	-1.167167	-0.408980	1.143533
H	-0.309522	0.163412	1.217019
C	-3.305177	-0.756302	0.212701
H	-3.637505	-1.243702	1.130822
O	-4.360179	-0.068337	-0.332112
O	-2.791890	-1.732123	-0.683614
H	-3.549015	-2.172167	-1.081464
H	-4.015208	0.757343	-0.699495
S	1.715990	0.859768	-0.045559
O	1.044187	0.746524	1.267167
O	2.990872	0.186476	-0.062438
O	2.021467	2.359681	-0.258105
O	0.805179	0.435701	-1.106458
H	1.150363	2.862729	-0.254808
H	0.352274	-1.172692	-0.991270
N	0.133624	-2.155847	-0.694302
H	0.632464	-2.798678	-1.302666

H	-0.879872	-2.288053	-0.690886
H	0.534958	-2.244133	0.267404
O	1.612194	-2.108748	1.630872
H	1.649287	-1.167771	1.853495
H	2.432552	-2.282637	1.152170
O	2.916975	-2.393609	-0.941194
H	3.718564	-2.699342	-1.368225
H	3.046615	-1.437808	-0.783161
O	-0.344385	3.426977	-0.258729
H	-0.610387	3.712962	-1.135422
H	-0.939033	2.687285	-0.040245

Table S52. Cartesian coordinate of $(GW)_1(SA)_1A_1W_4$.

Atoms	X	Y	Z
C	2.099070	-0.786610	0.589820
O	1.993017	-1.583289	-0.319777
O	1.323680	-0.706451	1.634160
H	0.490555	-1.261844	1.502324
C	3.153999	0.324476	0.540727
H	3.639525	0.432556	1.509259
O	4.089270	0.048981	-0.431019
O	2.465182	1.529758	0.309014
H	2.144330	1.530470	-0.613201
H	3.722927	-0.636292	-1.005141
S	-1.220662	-1.366799	-0.305046
O	-0.919852	-1.835531	1.051896
O	-2.611900	-1.451486	-0.654816
O	-0.485471	-2.346647	-1.286246
O	-0.648884	-0.039306	-0.520472

H	0.461780	-2.347360	-1.041257
H	-0.639655	2.526537	-1.640568
N	-0.201581	2.080256	1.369097
H	-0.078533	2.829979	2.041556
H	0.706344	1.637907	1.180340
H	-0.898466	1.385257	1.724843
O	-2.305486	0.492203	2.160231
H	-2.088125	-0.446725	2.086674
H	-2.886637	0.679115	1.406618
O	-3.447440	1.141280	-0.419740
H	-4.362932	1.316586	-0.646061
H	-3.265442	0.217535	-0.682512
O	-1.271216	2.879496	-0.999810
H	-2.026929	2.267699	-0.998883
H	-0.580444	2.459047	0.460296
O	0.991647	1.345514	-2.046903
H	1.285498	1.048617	-2.910118
H	0.419069	0.644521	-1.672539

Table S53. Cartesian coordinate of $(GW)_1(SA)_1A_1W_5$.

Atoms	X	Y	Z
C	2.174590	-1.104255	0.519043
O	2.066035	-1.634525	-0.567011
O	1.308911	-1.174688	1.494313
H	0.444469	-1.575631	1.171537
C	3.341702	-0.162991	0.832018
H	3.729742	-0.356142	1.830818
O	4.343761	-0.320765	-0.100307
O	2.811750	1.138117	0.856602

H	2.605046	1.392221	-0.061481
H	3.966799	-0.772405	-0.866126
S	-1.087543	-1.022259	-0.733546
O	-0.959571	-1.854309	0.465467
O	-2.447090	-0.845909	-1.177935
O	-0.381405	-1.817027	-1.891047
O	-0.358446	0.230707	-0.582083
H	0.530796	-2.006987	-1.594220
H	0.331696	2.952456	-1.144640
N	0.015065	1.754044	1.733631
H	0.204835	2.305892	2.563487
H	0.775635	1.086820	1.584841
H	-0.919416	1.275810	1.810632
O	-2.564878	0.988374	1.738012
H	-2.972394	0.101149	1.757585
H	-2.827578	1.372007	0.888773
O	-2.834400	1.904008	-0.975389
H	-3.610061	2.246029	-1.423519
H	-2.740067	0.971418	-1.242572
O	-0.357410	3.243884	-0.533239
H	-1.175534	2.817192	-0.838131
H	-0.047933	2.374777	0.886811
O	1.683758	1.555348	-1.669309
H	2.063037	1.330230	-2.520614
H	0.966009	0.916767	-1.488365
O	-3.619451	-1.571510	1.472526
H	-3.907737	-1.496064	0.556782
H	-2.752375	-1.987861	1.378568

Table S54. Cartesian coordinate of (**GW**)$_1$**A**$_2$.

Atoms	X	Y	Z
C	-0.754971	0.119275	-0.147947
O	-1.248187	1.106531	0.346824
O	-1.416429	-0.929907	-0.568306
H	-2.393714	-0.798866	-0.370441
C	0.760825	-0.004814	-0.310944
H	1.000281	-0.442659	-1.283548
O	1.335971	1.266553	-0.283483
O	1.183123	-0.818783	0.730921
H	2.144487	-0.938542	0.611217
H	0.783099	1.810276	0.293301
N	-3.933884	-0.253910	0.138630
H	-3.581304	0.632959	0.487963
H	-4.369502	-0.744467	0.909788
H	-4.650263	-0.060453	-0.549908
N	3.891855	-0.403739	0.017518
H	3.540276	0.528205	-0.182871
H	4.362304	-0.745299	-0.810889
H	4.587594	-0.319527	0.748055

Table S55. Cartesian coordinate of (**GW**)$_1$**A**$_2$**W**$_1$.

Atoms	X	Y	Z
C	-0.242799	-0.138444	-0.223019
O	-0.840886	0.899910	-0.020134
O	-0.774692	-1.312397	-0.365598
H	-1.795213	-1.302022	-0.235925
C	1.285479	-0.135635	-0.304062
H	1.620450	-0.814611	-1.091973

O	1.738406	1.138514	-0.648796
O	1.721372	-0.550013	0.946613
H	2.694325	-0.608255	0.889242
H	1.130413	1.770784	-0.244446
N	-3.396030	-1.376221	-0.016920
H	-3.725397	-0.438660	0.215617
H	-3.650551	-1.998509	0.740538
H	-3.895440	-1.683659	-0.842774
N	4.415146	-0.145066	0.178297
H	4.016545	0.655667	-0.303389
H	4.922030	-0.697361	-0.501766
H	5.089583	0.203692	0.847937
O	-3.538636	1.517158	0.276110
H	-2.577472	1.407229	0.179519
H	-3.663672	2.253803	0.874711

Table S56. Cartesian coordinate of $(GW)_1(SA)_2$.

Atoms	X	Y	Z
C	-0.170884	2.445085	-0.394854
O	-1.194486	3.198631	-0.965419
H	0.667685	3.072997	-0.083058
C	-0.769623	1.793141	0.865421
O	-0.109944	1.044520	1.555163
O	-2.002212	2.083757	1.164312
H	-2.389463	2.621060	0.453423
O	0.338682	1.486323	-1.256843
H	-0.921755	3.519340	-1.829688
H	-0.297462	0.741064	-1.306298
S	-1.967289	-1.465979	-0.196178

O	-1.655864	-0.193504	-0.799471
O	-3.258555	-2.000981	-0.343660
O	-1.657546	-1.349947	1.326489
O	-0.961734	-2.524463	-0.701240
H	-1.016947	-0.638604	1.517249
H	-0.038165	-2.208920	-0.576072
S	2.536756	-0.596696	0.053299
O	1.236256	-1.200720	-0.071018
O	3.682712	-1.393842	0.215893
O	2.447716	0.414816	1.224435
O	2.768399	0.305291	-1.191230
H	1.504068	0.673132	1.384955
H	1.956223	0.834316	-1.357148

Table S57. Cartesian coordinate of $(GW)_1(SA)_2W_1$.

Atoms	X	Y	Z
C	-3.000065	-1.492552	0.096239
O	-3.307766	-0.368227	-0.198411
O	-3.828823	-2.365453	0.640072
H	-4.689459	-1.943503	0.774592
C	-1.588157	-2.056006	-0.110279
H	-1.610803	-3.143390	-0.068544
O	-1.078008	-1.691201	-1.328335
O	-0.854548	-1.534351	0.975131
H	0.100849	-1.704644	0.841844
H	-0.973024	-0.727479	-1.352820
S	0.017590	1.725896	0.252579
O	-0.026040	0.920619	-0.952396
O	1.314126	2.081575	0.724493

O	-0.798707	1.006826	1.335689
O	-0.770116	3.009334	0.050893
H	-0.818327	-0.001306	1.206503
H	-1.704297	2.794572	-0.324469
S	2.869147	-0.777293	-0.068595
O	1.725757	-1.058963	0.756107
O	3.878111	-1.740925	-0.246028
O	3.535336	0.511542	0.479010
O	2.348228	-0.363724	-1.475052
H	2.843367	1.174138	0.695511
H	1.487165	0.102868	-1.399791
O	-3.016936	2.317227	-0.858946
H	-3.150069	1.379779	-0.637853
H	-3.108791	2.388439	-1.812282

Table S58. Cartesian coordinate of $(GW)_1(SA)_2W_2$.

Atoms	X	Y	Z
C	-0.058462	2.492284	-0.593307
O	-1.292508	2.930556	-1.055362
H	0.669104	3.303505	-0.518597
C	-0.292828	1.947442	0.829343
O	0.632246	1.554327	1.503999
O	-1.512102	1.952667	1.293458
H	-2.147561	2.179519	0.590299
O	0.502714	1.522377	-1.419329
H	-1.238471	3.131042	-1.994077
H	-0.071501	0.728455	-1.352499
S	-2.463014	-0.679892	-0.198789
O	-1.101763	-0.311782	-0.529731

O	-3.477520	0.286144	-0.407041
O	-2.468274	-1.157148	1.249765
O	-2.813306	-1.936712	-1.024584
H	-1.508517	-1.188321	1.652413
H	-2.016179	-2.531069	-1.014949
S	2.917522	-0.507440	-0.131530
O	1.627001	-1.150525	-0.072303
O	4.089625	-1.284671	-0.155253
O	3.009759	0.473771	1.063743
O	2.929967	0.416416	-1.376626
H	2.151909	0.946714	1.212558
H	2.072102	0.904270	-1.453150
O	-0.147966	-1.140134	2.183496
H	0.023474	-0.235010	2.473960
H	0.464568	-1.268510	1.439771
O	-0.450828	-3.065041	-0.721779
H	0.256568	-2.404863	-0.716565
H	-0.036244	-3.928724	-0.709901

Table S59. Cartesian coordinate of $(\mathbf{GW})_1(\mathbf{SA})_2\mathbf{W}_3$.

Atoms	X	Y	Z
C	-0.111444	-2.447931	-0.643890
O	1.030228	-3.072018	-1.131503
H	-0.960707	-3.132663	-0.609648
C	0.141037	-1.984425	0.804577
O	-0.827495	-1.661337	1.476650
O	1.325736	-1.953715	1.295104
H	2.126574	-2.049859	0.653510
O	-0.504617	-1.375372	-1.448547

H	0.826828	-3.449141	-1.992486
H	0.131576	-0.639874	-1.329380
S	2.277175	1.275409	-0.181659
O	1.136871	0.456168	-0.524710
O	3.570507	0.766072	-0.497746
O	2.200731	1.581925	1.307091
O	2.133604	2.627599	-0.886846
H	1.284648	1.298180	1.737568
H	1.163922	2.928354	-0.845842
S	-3.072044	0.350474	-0.101486
O	-1.833961	1.034484	0.214180
O	-4.279707	1.072290	-0.089446
O	-3.188933	-0.853472	0.851540
O	-2.909828	-0.283372	-1.504847
H	-2.285584	-1.231875	1.083303
H	-2.029248	-0.737558	-1.570794
O	0.036091	0.916711	2.317736
H	0.041597	-0.015193	2.572792
H	-0.664701	0.970784	1.644787
O	-0.352465	3.187882	-0.752386
H	-0.909156	2.425548	-0.518512
H	-0.703039	3.944248	-0.277713
O	3.418349	-1.986145	-0.098489
H	3.201293	-2.335365	-0.966975
H	3.675424	-1.057167	-0.236648

Table S60. Cartesian coordinate of $(GW)_1(SA)_2W_4$.

Atoms	X	Y	Z
C	0.255851	-2.263394	-0.569567

O	1.456077	-2.391871	-1.235809
H	-0.165064	-3.264804	-0.469046
C	0.421697	-1.711557	0.866139
O	-0.537797	-1.341776	1.516342
O	1.605283	-1.695813	1.408718
H	2.418735	-1.879818	0.823793
O	-0.680060	-1.487684	-1.253161
H	1.813289	-1.516632	-1.465910
H	-0.396578	-0.557622	-1.165366
S	2.087097	1.059798	-0.647069
O	0.722344	0.614426	-0.384702
O	2.857036	0.131210	-1.442588
O	2.763921	1.416637	0.602013
O	1.963301	2.358308	-1.499317
H	2.023843	1.103209	1.798725
H	1.109889	2.795330	-1.275901
S	-3.323268	-0.087470	-0.172544
O	-2.211316	0.837788	-0.228112
O	-4.631866	0.415369	-0.048120
O	-3.040626	-1.074126	0.975452
O	-3.278979	-0.967662	-1.450085
H	-2.053703	-1.219706	1.124069
H	-2.376256	-1.351987	-1.540820
O	1.390268	0.864931	2.594980
H	1.317192	-0.104848	2.595840
H	0.442945	1.279156	2.337943
O	-0.535389	3.125797	-0.678988
H	-1.052689	2.312319	-0.798155
H	-1.083997	3.845196	-1.001237

O	-0.740185	1.911933	1.929470
H	-1.271216	1.302906	1.388182
H	-0.535431	2.623896	1.304284
O	3.862219	-1.887709	0.240000
H	3.873306	-1.089867	-0.314558
H	3.935331	-2.622354	-0.376226

Table S61. Cartesian coordinate of $(GW)_1(SA)_2W_5$.

Atoms	X	Y	Z
C	0.677070	-2.410441	0.015926
O	1.806521	-2.475771	-0.778208
H	0.526532	-3.410897	0.425819
C	0.866236	-1.467907	1.222662
O	-0.104361	-0.962278	1.785063
O	2.043712	-1.253057	1.685647
H	2.863911	-1.584274	1.160205
O	-0.482879	-2.076087	-0.670420
H	2.001854	-1.598982	-1.144675
H	-0.464626	-1.129720	-0.894349
S	2.215893	1.020214	-0.747453
O	0.914604	0.368244	-0.654134
O	3.267539	0.142041	-1.199864
O	2.544806	1.711258	0.502719
O	2.086327	2.112283	-1.855682
H	1.575904	1.621290	1.540012
H	1.177644	2.485159	-1.817152
S	-2.978677	0.201052	0.088560
O	-1.925712	0.312824	-0.891375
O	-3.419012	1.417202	0.688243

51

O	-2.557752	-0.821099	1.155672
O	-4.193689	-0.494366	-0.526819
H	-1.556034	-0.898239	1.313226
H	-3.889394	-1.395230	-0.889923
O	0.800923	1.564234	2.252143
H	0.509505	0.626352	2.294811
H	0.000866	2.121052	1.891909
O	-0.552958	2.688981	-1.469851
H	-0.880867	1.776380	-1.358088
H	-1.147358	3.117404	-2.090683
O	-1.076448	2.910544	1.286710
H	-1.963346	2.516166	1.289856
H	-0.872331	3.050688	0.346867
O	4.232304	-1.763126	0.540442
H	4.216321	-0.994206	-0.057710
H	4.161702	-2.524945	-0.042919
O	-3.134031	-2.696359	-1.300465
H	-2.203871	-2.627670	-1.017690
H	-3.110861	-2.904253	-2.237328

Table S62. Cartesian coordinate of $(GW)_1(SA)_2W_6$.

Atoms	X	Y	Z
C	-0.478912	2.385900	-0.117952
O	-1.590565	2.404655	-0.941379
H	-0.342162	3.406280	0.244459
C	-0.694188	1.496386	1.125518
O	0.268632	1.001971	1.721766
O	-1.875887	1.297188	1.560863
H	-2.716208	1.722260	1.063319

O	0.698256	2.026775	-0.763587
H	-1.802796	1.509029	-1.252601
H	0.683670	1.072245	-0.949749
S	-1.870575	-1.090786	-0.816099
O	-0.567374	-0.477742	-0.614604
O	-2.833305	-0.211331	-1.441078
O	-2.379416	-1.674794	0.431232
O	-1.657483	-2.267797	-1.818986
H	-1.419728	-1.550709	1.556876
H	-0.724374	-2.576151	-1.749930
S	3.222084	-0.166620	0.162614
O	2.245170	-0.321708	-0.888188
O	3.632500	-1.362224	0.823818
O	2.719225	0.876270	1.167453
O	4.468431	0.529993	-0.388311
H	1.704393	0.936006	1.288122
H	4.169305	1.412759	-0.794631
O	-0.670707	-1.463600	2.267138
H	-0.377707	-0.520128	2.264356
H	0.146105	-2.027650	1.935896
O	0.973839	-2.739571	-1.389983
H	1.325008	-1.830092	-1.316178
H	1.586332	-3.227839	-1.945327
O	1.249087	-2.798781	1.401503
H	2.133901	-2.402048	1.452111
H	1.111608	-2.964029	0.452843
O	-3.962105	2.161427	0.600712
H	-4.510337	1.347476	0.466833
H	-3.791114	2.535673	-0.269384

O	3.379697	2.679230	-1.277468
H	2.440058	2.583211	-1.036551
H	3.392048	2.863266	-2.219442
O	-5.125262	-0.192909	0.166289
H	-4.859219	-0.818689	0.846347
H	-4.516165	-0.382516	-0.564534

Table S63. Cartesian coordinate of $(GW)_1(SA)_2W_7$.

Atoms	X	Y	Z
C	-0.317957	2.408380	-0.152723
O	-1.367569	2.460594	-1.061997
H	-0.211981	3.412293	0.259917
C	-0.638706	1.446382	1.017323
O	0.338820	0.868842	1.590867
O	-1.815632	1.298669	1.351875
H	-3.084353	2.284549	0.644423
O	0.898015	2.085875	-0.752057
H	-1.495446	1.565435	-1.407852
H	0.933511	1.132394	-0.936653
S	-1.741059	-1.232237	-1.082696
O	-0.601499	-0.340333	-1.006029
O	-2.940480	-0.612410	-1.614148
O	-1.993745	-1.903478	0.199710
O	-1.379588	-2.341117	-2.113034
H	-0.939594	-1.713293	1.283415
H	-0.431852	-2.586896	-1.975848
S	3.352894	-0.067342	0.275553
O	2.355719	-0.320701	-0.744415
O	3.881681	-1.225350	0.923700

O	2.778118	0.924358	1.277620
O	4.529190	0.703586	-0.322917
H	1.724111	0.953090	1.324418
H	4.195631	1.597606	-0.690164
O	-0.250494	-1.545422	2.012420
H	-0.011714	-0.549605	1.956087
H	0.587864	-2.115484	1.779348
O	1.218776	-2.704503	-1.484749
H	1.555269	-1.799230	-1.323166
H	1.830897	-3.112388	-2.102697
O	1.710470	-2.936581	1.315822
H	2.562736	-2.467160	1.340945
H	1.559924	-3.126267	0.376420
O	-3.928359	2.575397	0.233047
H	-4.517129	1.234235	0.029994
H	-3.642318	3.011607	-0.575744
O	3.477494	2.875126	-1.133996
H	2.522401	2.748124	-0.967575
H	3.561809	3.122948	-2.057218
O	-4.738789	0.220945	0.004112
H	-4.412202	-0.147602	0.911400
H	-4.104926	-0.171420	-0.678331
O	-3.675183	-0.607018	2.141316
H	-3.281749	-1.436748	1.843572
H	-2.925850	0.016679	2.154810

Table S64. Cartesian coordinate of $(SA)_1A_1$.

Atoms	X	Y	Z
S	0.598701	-0.112566	0.085247

Atoms	X	Y	Z
O	1.008723	1.400067	-0.155157
O	-0.387978	-0.388928	-1.057140
O	1.757160	-0.906230	-0.109542
O	-0.102665	-0.107432	1.324252
H	1.743999	1.429704	-0.779566
H	-1.367686	-0.203503	-0.740444
N	-2.731944	0.043273	-0.051253
H	-2.432364	0.084441	0.919179
H	-3.405948	-0.706646	-0.145142
H	-3.195540	0.914342	-0.278505

Table S65. Cartesian coordinate of $(SA)_1A_1W_1$.

Atoms	X	Y	Z
S	0.029350	0.441626	-0.025850
O	-0.987181	1.276040	0.519351
O	1.093457	1.010728	-0.790215
O	-0.620434	-0.658931	-0.885415
O	0.648687	-0.341693	1.172007
H	-1.601887	-0.808830	-0.579182
H	1.545642	-0.674998	0.910661
N	-3.067373	-0.785780	-0.012617
H	-3.037943	0.107606	0.471473
H	-3.301177	-1.503564	0.662167
H	-3.807254	-0.749736	-0.702804
O	3.021078	-0.817239	0.076781
H	3.185121	-1.586031	-0.472995
H	2.774652	-0.101249	-0.527467

Table S66. Cartesian coordinate of $(SA)_1A_1W_2$.

Atoms	X	Y	Z
N	2.044363	0.277479	1.105483
H	1.103437	-0.004915	1.467715
H	1.874615	1.084854	0.455997
H	2.382947	-0.531876	0.549562
O	1.226768	2.238229	-0.635138
H	0.268176	2.127766	-0.476990
H	1.346110	1.934708	-1.539087
O	2.205669	-1.780625	-0.692199
H	2.197148	-2.731129	-0.571648
H	1.286980	-1.519607	-0.909225
S	-1.023406	-0.086326	0.061649
O	-2.411290	-0.850412	-0.046405
O	-0.536676	-0.483103	1.369583
O	-1.323639	1.324624	-0.068977
O	-0.181819	-0.569818	-1.022982
H	-2.911451	-0.478974	-0.782679
H	2.683886	0.526872	1.850543

Table S67. Cartesian coordinate of $(\mathbf{SA})_1\mathbf{A}_1\mathbf{W}_3$.

Atoms	X	Y	Z
S	0.254957	1.059105	0.012842
O	-0.604198	0.360729	-0.927425
O	-0.315307	2.545020	-0.032655
O	1.639067	1.146017	-0.385212
O	0.078929	0.594079	1.381843
H	0.316123	3.133823	0.397211
N	-1.259210	-1.748181	1.089926
H	-2.147853	-1.463584	0.645664

H	-0.801133	-0.876407	1.436853
H	-1.412278	-2.419494	1.832896
H	-0.599145	-2.122926	0.347685
O	-3.163124	-0.479953	-0.485047
H	-3.884454	0.141533	-0.380806
H	-2.390236	0.031596	-0.784293
O	2.887350	-1.299626	0.023415
H	3.238317	-1.349901	0.913580
H	2.604368	-0.375376	-0.095691
O	0.496228	-2.331211	-0.853770
H	0.259616	-1.555073	-1.379264
H	1.400282	-2.133042	-0.537975

Table S68. Cartesian coordinate of $(SA)_1A_1W_4$.

Atoms	X	Y	Z
S	1.021668	0.729642	0.029082
O	2.424803	1.461399	0.172442
O	0.955900	-0.079209	1.225014
O	0.023902	1.779591	-0.041935
O	1.094544	-0.049191	-1.199728
H	2.562715	2.033371	-0.592010
N	-1.141825	-2.191564	-0.020662
H	-0.118645	-2.398894	0.005706
H	-1.672658	-3.054754	-0.058663
H	-1.412225	-1.624328	0.819362
H	-1.352480	-1.591250	-0.856187
H	1.817074	-2.094100	0.779248
O	1.622129	-2.581027	-0.030966
H	1.739237	-1.895215	-0.705764

Atoms	X	Y	Z
H	-3.167239	2.247406	-0.028664
O	-2.627055	1.455392	-0.032744
H	-1.691335	1.744539	-0.017268
H	-2.249781	0.285253	1.476482
O	-1.762844	-0.401254	1.956682
H	-0.856950	-0.063828	2.026378
H	-2.133967	0.324638	-1.549780
O	-1.619694	-0.363169	-1.997963
H	-0.711140	-0.026423	-2.025949

Table S69. Cartesian coordinate of $(\mathbf{SA})_1\mathbf{A}_1\mathbf{W}_5$.

Atoms	X	Y	Z
S	0.410341	1.108914	-0.187593
O	-0.622145	0.414410	0.561478
O	-0.248661	2.547644	-0.394768
O	0.597709	0.557015	-1.523415
O	1.647599	1.312455	0.523557
H	0.399496	3.140756	-0.793452
N	-0.707533	-1.929660	-1.149203
H	-0.454511	-1.024529	-1.566777
H	-0.719436	-2.654196	-1.858892
H	-1.647174	-1.850805	-0.709933
H	0.062944	-2.122752	-0.431072
O	-3.317952	0.974567	0.450887
H	-2.351528	0.989555	0.556207
H	-3.536943	1.731076	-0.095606
O	1.096082	-0.590674	2.656633
H	1.631621	0.125990	2.293656
H	0.209940	-0.323226	2.385103

Atoms	X	Y	Z
O	1.368854	-2.284242	0.462806
H	1.312331	-1.798372	1.308580
H	2.103286	-1.865445	-0.023700
O	3.136935	-0.726134	-1.054758
H	3.420663	-0.080032	-0.400541
H	2.395357	-0.272931	-1.481146
O	-3.317032	-1.632853	-0.252883
H	-3.446711	-0.685183	-0.037151
H	-3.723182	-2.122409	0.464325

Table S70. Cartesian coordinate of $(SA)_2$.

Atoms	X	Y	Z
S	2.035365	0.073179	-0.114230
O	1.423634	0.890121	1.038482
O	1.067003	-0.084348	-1.156776
O	2.180490	-1.369640	0.491648
O	3.310912	0.603152	-0.396157
H	0.462447	0.657267	1.158023
H	2.959353	-1.415425	1.062894
S	-2.035370	-0.073179	0.114229
O	-2.180420	1.369656	-0.491629
O	-1.067011	0.084289	1.156788
O	-1.423664	-0.890133	-1.038488
O	-3.310943	-0.603099	0.396135
H	-2.959260	1.415482	-1.062902
H	-0.462472	-0.657301	-1.158027

Table S71. Cartesian coordinate of $(SA)_2W_1$.

Atoms	X	Y	Z

S	-1.460321	-0.680851	-0.062989
O	-1.136151	-0.665008	1.445079
O	-0.472080	-1.435517	-0.763813
O	-1.230284	0.803924	-0.498788
O	-2.835220	-0.998806	-0.195667
H	-0.178088	-0.423888	1.558214
H	-2.069308	1.338574	-0.309121
S	2.227427	0.247502	0.099560
O	1.562981	1.233111	-0.910716
O	3.561877	0.645549	0.279774
O	2.234237	-1.106578	-0.654776
O	1.349547	0.136318	1.234572
H	0.590132	1.204536	-0.844447
H	1.315188	-1.433923	-0.760740
O	-3.552470	1.774271	-0.054426
H	-3.803513	2.238350	0.748015
H	-3.987598	0.911817	-0.026967

Table S72. Cartesian coordinate of $(SA)_2W_2$.

Atoms	X	Y	Z
S	2.168579	-0.112973	-0.007448
O	1.940366	-1.621859	0.214116
O	1.514025	0.180884	-1.382703
O	1.416872	0.595317	1.002887
O	3.550011	0.121570	-0.119939
H	0.973769	-1.812646	0.341597
H	0.524216	0.111239	-1.331587
S	-1.603000	-0.780715	0.014263
O	-2.877166	-1.434309	-0.637785

O	-0.698083	-1.853290	0.346916
O	-1.110572	0.095335	-1.044099
O	-2.073729	-0.033428	1.172412
H	-3.235365	-2.115325	-0.053316
O	-0.654928	2.027842	1.398255
H	-0.884292	2.503744	0.529457
H	-1.298818	1.225178	1.432128
H	0.242212	1.592962	1.272083
H	-1.441827	1.961393	-1.277186
O	-1.385668	2.850406	-0.889942
H	-0.898160	3.404724	-1.503149

Table S73. Cartesian coordinate of $(SA)_2W_3$.

Atoms	X	Y	Z
S	1.658037	-0.904255	-0.000025
O	0.838390	-0.888392	-1.207484
O	0.838468	-0.888418	1.207495
O	2.442101	-2.267695	-0.000040
O	2.714768	0.073775	-0.000068
H	1.222953	2.380545	0.828867
S	-2.264842	-0.178316	0.000009
O	-1.775428	-0.991869	-1.221765
O	-1.775326	-0.991974	1.221667
O	-1.550522	1.082079	0.000035
O	-3.670289	-0.170368	0.000065
H	-0.777973	-1.005838	1.261875
H	-0.778083	-1.005806	-1.261979
O	0.322950	1.907600	-1.904016
H	-0.523423	1.732554	-1.458032

H	0.641774	1.027273	-2.148208
O	1.836727	2.523434	-0.000012
H	2.394823	1.699606	-0.000033
H	1.222896	2.380540	-0.828872
H	1.828535	-3.013516	0.000466
O	0.323018	1.907579	1.904090
H	-0.523369	1.732502	1.458149
H	0.641872	1.027265	2.148286

Table S74. Cartesian coordinate of $(\mathbf{SA})_2\mathbf{W}_4$.

Atoms	X	Y	Z
S	-1.856780	0.565211	-0.179448
O	-1.089496	0.348264	1.093117
O	-0.651010	-2.155711	1.247215
H	-0.839520	-1.161273	1.349591
O	-3.174895	0.006770	-0.093148
O	-1.130336	-0.332177	-1.234322
O	-2.693953	-2.715575	-0.126691
H	-1.430980	-2.498295	0.664192
O	0.842681	1.943739	1.520908
H	1.599854	1.290926	1.351121
S	2.136868	-0.625984	-0.183789
O	1.395848	0.229068	-1.096981
O	1.536258	-1.944854	-0.045200
O	2.443307	0.020849	1.074947
H	-0.157231	-0.104742	-1.284024
O	-1.754479	1.941623	-0.582383
H	-2.517389	-2.938576	-1.044903
H	-3.089280	-1.820655	-0.154284

Atoms	X	Y	Z
H	0.224191	-2.178546	0.732974
H	0.007917	1.367084	1.423831
H	0.784161	2.652394	0.777463
O	3.557789	-0.863657	-0.818833
H	3.469894	-1.346774	-1.650175
H	0.189432	4.453139	-0.187537
O	0.426665	3.542253	-0.375567
H	-0.389494	3.092955	-0.670967

Table S75. Cartesian coordinate of (**SA**)$_2$**W**$_5$.

Atoms	X	Y	Z
S	2.536717	0.064430	-0.144640
O	1.752639	-0.479030	0.944371
O	4.025402	-0.184773	0.318889
O	2.403568	1.498181	-0.318429
O	2.373718	-0.665927	-1.393042
H	4.636287	0.164279	-0.342804
S	-2.363018	-0.285407	0.029788
O	-1.551791	-0.284529	-1.183643
O	-3.674454	-1.033113	-0.450936
O	-2.751258	1.038808	0.454585
O	-1.799157	-1.076146	1.106822
H	-4.315492	-1.056725	0.270701
O	0.262195	-2.073250	-1.476572
H	1.123359	-1.535490	-1.533376
H	0.276135	-2.518797	-0.530250
H	-0.493332	-1.403487	-1.443762
O	0.250077	2.712194	0.388380
H	1.112805	2.319203	0.057005

H	-0.039397	2.095425	1.175056
H	-0.449489	2.701732	-0.366251
O	-0.178456	1.091704	2.242098
H	-1.001142	0.590814	2.158559
H	0.523319	0.457527	2.016926
O	-1.524406	2.634803	-1.414624
H	-2.259128	2.325400	-0.857404
H	-1.340823	1.860654	-1.961264
O	0.285602	-2.892285	0.884427
H	-0.531905	-2.449338	1.171112
H	0.990189	-2.308650	1.204776

Table S76. Cartesian coordinate of (**SA**)$_2$**W**$_6$.

Atoms	X	Y	Z
S	2.388277	-0.052619	-0.085444
O	1.703805	-0.687203	1.017423
O	3.912168	-0.222106	0.292051
O	2.149133	1.375526	-0.203850
O	2.203069	-0.730280	-1.360713
H	4.466298	0.186319	-0.385422
S	-2.268250	-0.437175	-0.033414
O	-1.489260	-0.584267	-1.260093
O	-3.668069	-1.032379	-0.470677
O	-2.484481	0.930074	0.363337
O	-1.782157	-1.265632	1.054985
H	-4.297093	-0.949952	0.257157
O	0.288934	-2.413613	-1.430647
H	1.103099	-1.813692	-1.483694
H	0.295839	-2.816106	-0.462177

H	-0.491639	-1.772193	-1.443715
O	0.336158	2.692702	1.235845
H	1.091062	2.305939	0.729257
H	0.001695	1.920088	1.825241
H	-0.418791	2.992542	0.514302
O	-0.225593	0.638031	2.592955
H	-1.025297	0.179647	2.299102
H	0.496682	0.084739	2.254862
O	-1.314561	3.281850	-0.472987
H	-2.044288	2.673354	-0.275767
H	-0.876284	2.861806	-1.252582
O	0.270826	-3.123941	0.960341
H	-0.548295	-2.659113	1.206367
H	0.972768	-2.538095	1.281248
O	-0.025410	1.728955	-2.221613
H	-0.505097	0.904999	-2.057117
H	0.862413	1.574680	-1.876178

Table S77. Cartesian coordinate of $(SA)_2W_7$.

Atoms	X	Y	Z
S	2.624290	-0.104566	-0.155364
O	1.830762	-0.303430	-1.345772
O	4.087096	-0.452718	-0.632579
O	2.307579	-1.038104	0.920956
O	2.662739	1.263628	0.325012
H	4.712441	-0.304857	0.088436
S	-2.449013	-0.052676	-0.454121
O	-1.624871	0.837081	0.343279
O	-3.853412	0.683238	-0.432409

O	-2.645053	-1.364324	0.116808
O	-2.032020	-0.109189	-1.847561
H	-4.497299	0.165191	-0.931514
O	0.715761	2.926322	-0.121546
H	1.506231	2.365725	0.113620
H	0.297954	2.453583	-0.969502
H	0.083742	2.960432	0.684184
O	0.406287	-2.818690	0.602603
H	1.190737	-2.219732	0.730950
H	0.059283	-2.639914	-0.359909
H	-0.309796	-2.577659	1.335169
O	-0.165552	-2.264179	-1.770742
H	-0.965272	-1.732208	-1.912059
H	0.570569	-1.653656	-1.928057
O	-1.255734	-2.140008	2.326160
H	-1.985347	-1.846578	1.750340
H	-0.871575	-1.324138	2.688735
O	0.032136	1.718980	-2.167675
H	-0.783372	1.184951	-2.120770
H	0.747540	1.064021	-2.179213
O	0.160058	0.304444	2.379040
H	-0.304713	0.376084	1.527691
H	1.058484	0.024001	2.160072
O	-0.794821	2.939868	1.928861
H	-1.579553	2.490656	1.585923
H	-0.382129	2.266620	2.492183

Table S78. Cartesian coordinate of (**SA**)$_2$**A**$_1$.

Atoms	X	Y	Z

S	1.780537	-0.350791	-0.049136
O	2.395462	0.755681	-0.764877
O	1.080155	0.142334	1.140082
O	2.963043	-1.265437	0.453993
O	0.987268	-1.244923	-0.848949
H	1.426284	2.076968	-0.427545
H	3.664760	-0.718983	0.827862
S	-2.076443	-0.119175	-0.011823
O	-1.445033	-0.409398	1.369034
O	-3.477924	-0.145654	0.115487
O	-1.644788	-1.308567	-0.893008
O	-1.454162	1.076500	-0.540365
H	-0.452948	-0.256205	1.349764
H	-0.652732	-1.340057	-0.972091
N	0.631706	2.651699	-0.045424
H	-0.240934	2.080913	-0.198980
H	0.560393	3.559485	-0.492964
H	0.775564	2.751155	0.956084

Table S79. Cartesian coordinate of $(SA)_2A_1W_1$.

Atoms	X	Y	Z
S	-2.230852	0.044075	0.037008
O	-2.132880	-1.454101	-0.328047
O	-1.460518	0.791013	-0.926694
O	-1.509323	0.151411	1.405004
O	-3.589610	0.362270	0.224289
H	-1.180090	-1.718773	-0.419229
H	-0.520870	0.115357	1.285288
S	1.503940	-0.919523	-0.063789

O	0.477492	-1.895383	-0.348176
O	2.629944	-1.669478	0.753814
O	1.070545	0.112166	0.880012
O	2.134939	-0.362437	-1.239516
H	2.966321	-2.411618	0.235801
N	0.890747	2.083506	-1.405521
H	-0.065411	1.722676	-1.216725
H	1.243974	2.570076	-0.560303
H	1.486782	1.244484	-1.553070
O	1.995546	2.730985	1.032331
H	1.843375	1.808214	1.289401
H	1.796950	3.270161	1.799607
H	0.895236	2.690484	-2.217760

Table S80. Cartesian coordinate of $(\mathbf{SA})_2\mathbf{A}_1\mathbf{W}_2$.

Atoms	X	Y	Z
S	-2.439383	-0.166384	-0.148815
O	-2.303218	1.113452	-0.796023
O	-3.981338	-0.353243	0.157645
O	-2.118886	-1.325613	-0.950125
H	-4.358607	0.494614	0.421208
S	2.438468	-0.153992	-0.135130
O	2.213447	1.057162	-0.881832
O	1.749336	-0.198447	1.153183
O	3.962905	-0.148779	0.296145
O	2.225278	-1.371211	-0.897346
H	0.897224	-2.168100	-0.281492
O	-1.755410	-0.211648	1.151297
O	-0.017507	1.611482	1.538094

N	0.024068	-2.454620	0.227802
O	-0.015328	2.688398	-0.689642
H	0.024545	-1.955005	1.117965
H	-0.825126	-2.130545	-0.300859
H	4.512110	0.004725	-0.482602
H	-0.803200	2.261794	-1.065128
H	0.758501	2.238994	-1.069754
H	-0.795805	0.966091	1.462921
H	-0.017026	2.162366	0.630018
H	0.780805	0.997433	1.481615
H	-0.001487	-3.456429	0.383454

Table S81. Cartesian coordinate of $(SA)_2A_1W_3$.

Atoms	X	Y	Z
S	2.111424	-0.795585	-0.162589
O	3.576930	-1.030117	-0.703513
O	1.423566	-2.063947	-0.271836
O	2.334450	-0.342506	1.195481
O	1.512193	0.233219	-1.009120
H	3.538353	-1.479843	-1.556887
S	-1.782808	0.841269	-0.124000
O	-1.137087	-0.201916	-1.116391
O	-3.174308	0.492807	-0.134006
O	-1.147995	0.537831	1.190746
O	-1.436976	2.165144	-0.566668
H	-0.167682	-0.035574	-1.206409
N	-1.028694	-2.233870	1.010858
H	-1.897138	-2.415723	0.459925
H	-0.963961	-2.860319	1.806074

H	-0.174724	-2.310606	0.427070
H	-1.075592	-1.244822	1.324310
O	0.991070	1.804851	1.657194
H	1.623568	1.027434	1.566538
H	1.121455	2.393767	0.803377
H	0.070674	1.368818	1.541836
H	-3.477670	-1.276993	-0.430696
O	-3.390245	-2.248016	-0.383006
H	-4.260398	-2.588009	-0.169890
H	1.578234	2.326608	-1.042924
O	1.173619	3.031209	-0.517968
H	0.226131	2.972944	-0.740205

Table S82. Cartesian coordinate of $(SA)_2A_1W_4$.

Atoms	X	Y	Z
S	-1.861767	0.740978	-0.022891
O	-0.981151	0.498306	1.128133
O	-3.033826	-0.115978	-0.006037
O	-1.047503	0.235867	-1.279426
O	-2.133015	2.139164	-0.218836
H	-0.066415	0.384458	-1.145889
O	-0.409036	-2.058327	2.002146
H	0.427782	-2.207378	1.537107
H	-1.518537	-2.411691	1.082293
H	-0.514729	-1.091497	1.955617
O	-2.233493	-2.511813	0.333750
H	-1.685681	-2.646588	-0.518988
H	-2.667725	-1.592435	0.230257
O	0.279527	3.333705	-1.032289

Atoms	X	Y	Z
H	0.698681	2.723828	-1.647299
H	0.809390	2.870691	0.502496
H	-0.654755	3.065039	-0.986613
S	2.126457	-0.429454	-0.069624
O	1.493676	0.569581	-0.934273
O	1.455944	-1.716377	-0.145334
O	2.369366	0.048650	1.264734
O	3.581004	-0.647374	-0.654054
H	3.528971	-1.088708	-1.510597
N	0.910172	2.425321	1.450200
H	0.064772	1.832610	1.567997
H	1.700693	1.762643	1.454490
H	-0.977569	-1.780130	-2.141735
O	-0.702152	-2.594312	-1.703181
H	0.139566	-2.350980	-1.276538
H	0.994580	3.119800	2.183595

Table S83. Cartesian coordinate of $(SA)_2A_1W_5$.

Atoms	X	Y	Z
S	1.774147	0.949562	-0.495563
O	3.141241	0.696707	-0.118981
O	1.428582	-0.275287	-1.434493
O	0.828721	0.866380	0.625362
H	0.493090	-0.199582	-1.730927
S	-1.918521	-0.766108	-0.856314
O	-1.217290	0.059056	-1.826592
O	-3.045476	-1.441979	-1.743219
O	-2.599857	0.023771	0.152484
H	-3.522158	-2.094602	-1.216294

N	-1.091681	2.694303	-0.704135
H	-1.468731	1.836303	-1.125360
O	3.496002	-1.971344	-0.066112
H	2.110756	-2.326822	0.361888
H	3.682713	-2.234898	-0.970607
H	3.517993	-0.987831	-0.072516
O	0.745960	-0.961111	2.579862
H	-0.197747	-0.872065	2.802178
H	0.914907	-0.183278	2.007542
O	1.179240	-2.541252	0.750195
H	0.994115	-1.936882	1.610866
O	-1.898918	-0.107273	2.748681
H	-2.624619	-0.401789	3.301981
H	-2.204375	-0.175446	1.819824
O	-0.954786	2.505288	2.025717
H	-0.077665	2.127531	1.870907
H	-1.440887	1.775067	2.436145
O	1.545643	2.159278	-1.260077
H	-0.073831	2.697282	-0.940134
O	-1.131253	-1.847393	-0.306368
H	0.460537	-2.285653	0.126117
H	-1.559899	3.514284	-1.073139
H	-1.194897	2.634280	0.338841

Table S84. AIM topological parameters for the stable clusters obtained at the M06-2X/6-311++G(3df,3pd) level (in a.u.).

Clusters	Bonds	r	ρ	$\nabla^2\rho$
$(\mathbf{GA})_1 \cdot \mathbf{A}_1$	C=O...H-N	2.460	0.0115	0.0392

	C-O-H...N-H	1.683	0.0548	0.1281
$(GW)_1 \cdot A_1$	C=O...H-N	2.428	0.0120	0.0403
	C-O-H...N-H	1.695	0.0531	0.1277
$(GA)_1 \cdot A_1 \cdot W_1$	C=O...H-O-H	1.840	0.0293	0.1139
	C-O-H...N-H	1.582	0.0712	0.1084
$(GW)_1 \cdot A_1 \cdot W_1$	C=O...H-O-H	1.831	0.0298	0.1164
	C-O-H...N-H	1.598	0.0684	0.1134
$(GA)_1 \cdot (SA)_1$	C=O...H-O-S	1.571	0.0582	0.1761
	C-O-H...O=S	1.668	0.0432	0.1619
$(GW)_1 \cdot (SA)_1$	C=O...H-O-S	1.849	0.0274	0.1102
	O-H...O=S	1.839	0.0289	0.1127
	H-O...H-O-S	1.731	0.0398	0.1400
$(GA)_1 \cdot (SA)_1 \cdot W_1$	C=O...H-O-S	1.592	0.0552	0.1744
	C-O-H...O=S	1.654	0.0451	0.1652
$(GW)_1 \cdot (SA)_1 \cdot W_1$	C=O...H-O-S	1.712	0.0410	0.1479
	C-O-H...O=S	1.601	0.0531	0.1773
	H-O...H-O-H	1.907	0.0253	0.0959
$(GA)_1 \cdot (SA)_1 \cdot W_2$	C=O...H-O-S	1.603	0.0537	0.1728
	C-O-H...O=S	1.640	0.0472	0.1685
$(GW)_1 \cdot (SA)_1 \cdot W_2$	C=O...H-O-S	1.570	0.0584	0.1771
	C-O-H...O=S	1.656	0.0455	0.1640
$(GA)_1 \cdot (SA)_1 \cdot W_3$	C=O...H-O-S	1.736	0.0366	0.1446
	C-O-H...O=S	1.664	0.0447	0.1620
$(GW)_1 \cdot (SA)_1 \cdot W_3$	C=O...H-O-H	1.879	0.0267	0.1075
	C-O(H)...H-O-H	2.061	0.0181	0.0630
	O-H...O=S	1.728	0.0400	0.1484
$(GA)_1 \cdot (SA)_1 \cdot N_1$	C=O...H-O-S	1.622	0.0511	0.1694
	C-O-H...O=S	1.620	0.0495	0.1740
$(GW)_1 \cdot (SA)_1 \cdot N_1$	C=O...H-O-S	1.737	0.0387	0.1402

	C-O-H...O=S	1.554	0.0609	0.1815
	H-O...H-N-H	2.128	0.0165	0.0545
$(GA)_1 \cdot (SA)_1 \cdot N_1 \cdot W_1$	C=O...H-O-S	1.675	0.0451	0.1576
	C-O-H...O=S	1.571	0.0578	0.1790
$(GW)_1 \cdot (SA)_1 \cdot N_1 \cdot W_1$	C=O...H-O-S	1.869	0.0285	0.1020
	C-O-H...O=S	1.479	0.0775	0.1639
	H-O...H-N-H	1.994	0.0219	0.0760
$(GA)_1 \cdot (SA)_1 \cdot N_1 \cdot W_2$	C=O...H-O-H	1.889	0.0259	0.0988
	C-O-H...O=S	1.407	0.0927	0.1261
$(GW)_1 \cdot (SA)_1 \cdot N_1 \cdot W_2$	C=O...H-O-S	1.929	0.0250	0.0868
	C-O-H...O=S	1.486	0.0758	0.1695
	H-O...H-N-H	2.063	0.0192	0.0648
$(GA)_1 \cdot (SA)_1 \cdot N_1 \cdot W_3$	C=O...H-O-H	1.843	0.0287	0.1119
	C-O-H...O=S	1.461	0.0803	0.1589
$(GW)_1 \cdot (SA)_1 \cdot N_1 \cdot W_3$	C=O...H-O-H	1.831	0.0295	0.1152
	C-O-H...O=S	1.475	0.0769	0.1658
	H-O...H-N-H	1.991	0.0222	0.0771
$(GA)_1 \cdot (SA)_1 \cdot N_1 \cdot W_4$	C=O...H-O-H	2.125	0.0177	0.0583
	C-O-H...O=S	1.542	0.0644	0.1806
$(GW)_1 \cdot (SA)_1 \cdot N_1 \cdot W_4$	C=O...H-O-H	1.857	0.0183	0.0412
	C-O-H...O=S	1.588	0.0410	0.0584
	H-O...H-N-H	1.966	0.0201	0.0312
	O-H...O-H2	1.849	0.0293	0.0288
$(GA)_1 \cdot (SA)_2$	C=O...H-O-S	1.508	0.0690	0.1724
	C-O-H...O=S	1.698	0.0403	0.1521
$(GW)_1 \cdot (SA)_2$	C=O...H-O-S	1.912	0.0245	0.0884
	C=O...H-O-S	1.665	0.0455	0.1611
	H-O...H-O-S	1.747	0.0381	0.1384
$(GA)_1 \cdot (SA)_2 \cdot W_1$	C=O...H-O-S	1.532	0.0646	0.1760

	C-O-H...O=S	1.698	0.0402	0.1522
$(GW)_1 \cdot (SA)_2 \cdot W_1$	C=O...H-O-H	1.809	0.0284	0.1242
	O-H...O=S	1.943	0.0236	0.0863
	H-O...H-O-S	1.551	0.0642	0.1651
	O-H...O=S	1.751	0.0351	0.1427
$(GA)_1 \cdot (SA)_2 \cdot W_2$	C=O...H-O-S	1.549	0.0618	0.1768
	C-O-H...O=S	1.677	0.0429	0.1578
$(GW)_1 \cdot (SA)_2 \cdot W_2$	C=O...H-O-S	1.662	0.0444	0.1649
	C=O...H-O-H	2.124	0.0182	0.0573
	H-O...H-O-S	1.687	0.0439	0.1539
	O-H...O=S	1.679	0.0426	0.1677
$(GA)_1 \cdot (SA)_2 \cdot W_3$	C=O...H-O-S	1.599	0.0545	0.1736
	C-O-H...O=S	1.627	0.0492	0.1706
$(GW)_1 \cdot (SA)_2 \cdot W_3$	C=O...H-O-S	1.570	0.0576	0.1809
	C=O...H-O-H	2.160	0.0180	0.0560
	C-O-H...O-H2	1.496	0.0742	0.1572
	H-O...H-O-S	1.657	0.0476	0.1623
	O-H...O=S	1.691	0.0397	0.1637
$(GA)_1 \cdot (SA)_2 \cdot W_4$	C=O...H-O-S	1.582	0.0571	0.1753
	C-O-H...O=S	1.617	0.0508	0.1725
$(GW)_1 \cdot (SA)_2 \cdot W_4$	C=O...H-O-S	1.571	0.0579	0.1779
	C-O-H...O-H2	1.557	0.0636	0.1642
	C-O(H)...H-O-H	2.006	0.0222	0.0743
	O-H...O=S	1.799	0.0340	0.1277
	O-H...O=S	1.951	0.0247	0.0834
	H-O...H-O-S	1.726	0.0397	0.1458
$(GW)_1 \cdot (SA)_2 \cdot W_5$	C=O...H-O-S	1.590	0.0558	0.1742
	C-O-H...O=S	1.615	0.0510	0.1731

Table S85. The realistic hydration reaction conversion ratio (X_{GA}, %) of **GA**-based clusters at varying temperatures and ralative humidities.

$[SA]=10^6$ molecules cm^{-3}, $[A]=10^9$ molecules cm^{-3}, $[GA]=10^8$ molecules cm^{-3}		
Temperature (K)	Relative Humidity (%)	X_{GA} (%)
220	0	0.00
220	0.01	0.16
220	0.1	4.75
220	1	28.63
220	20	33.05
220	40	33.44
220	60	33.74
220	80	34.01
220	100	34.27
240	0	0.00
240	0.01	0.01
240	0.1	0.59
240	1	18.50
240	20	32.89
240	40	33.84
240	60	34.16
240	80	34.30
240	100	34.36
260	0	0.00
260	0.01	0.00
260	0.1	0.10
260	1	6.89
260	20	32.47
260	40	33.87
260	60	34.33
260	80	34.53
260	100	34.63
280	0	0.00
280	0.01	0.00
280	0.1	0.02
280	1	1.73
280	20	29.78
280	40	32.59
280	60	33.50
280	80	33.90
280	100	34.10
300	0	0.00
300	0.01	0.00

300	0.1	0.00
300	1	0.44
300	20	22.69
300	40	28.13
300	60	30.01
300	80	30.89
300	100	31.34

Table S86. The realistic hydration reaction conversion ratio (X_{GA}, %) of **GA**-based clusters at varying ammonia and sulfuric acid concentrations.

260K, RH=50%, [GA]=10^8 molecules cm^{-3}		
[A] (molecules cm^{-3})	[SA] (molecules cm^{-3})	X_{GA} (%)
10^7	10^4	0.52
10^7	10^5	4.93
10^7	10^6	34.15
10^7	10^7	83.85
10^7	10^8	98.13
10^8	10^4	0.52
10^8	10^5	4.93
10^8	10^6	34.15
10^8	10^7	83.85
10^8	10^8	98.13
10^9	10^4	0.52
10^9	10^5	4.93
10^9	10^6	34.15
10^9	10^7	83.85
10^9	10^8	98.13
10^{10}	10^4	0.52
10^{10}	10^5	4.93
10^{10}	10^6	34.17
10^{10}	10^7	83.86
10^{10}	10^8	98.13
10^{11}	10^4	0.52
10^{11}	10^5	4.97
10^{11}	10^6	34.33
10^{11}	10^7	83.96
10^{11}	10^8	98.13

Table S87. The formation rates (J, cm^{-3} s^{-1}) of $(\mathbf{GA/GW})_x \cdot (\mathbf{SA})_y \cdot \mathbf{A}_z$ clusters with the vabriations of the concentration of **GA** ([**GA**]) at different temperatures of 220, 240, 260, 280 and 300 K. [**SA**]=10^6 molecules cm^{-3}. [**A**]=10^9 molecules cm^{-3}. RH=50%.

[GA]	220 K	240 K	260 K	280 K	300 K
10^7	1.05×10^2	1.92×10^1	2.09×10^{-2}	5.59×10^{-5}	3.69×10^{-7}
10^8	1.13×10^2	1.92×10^1	2.09×10^{-2}	5.59×10^{-5}	3.69×10^{-7}
10^9	2.04×10^2	1.94×10^1	2.09×10^{-2}	5.59×10^{-5}	3.69×10^{-7}
10^{10}	2.89×10^3	2.10×10^1	2.10×10^{-2}	5.59×10^{-5}	3.69×10^{-7}
10^{11}	2.09×10^5	4.24×10^1	2.17×10^{-2}	5.61×10^{-5}	3.69×10^{-7}

Table S88. The formation rates (J, cm^{-3} s^{-1}) of $(\mathbf{GA/GW})_x \cdot (\mathbf{SA})_y \cdot \mathbf{A}_z$ clusters with the vabriations of the concentration of **GA** ([**GA**]) at different relative humidities (RH) of 20%, 40%, 60%, 80% and 100%. [**SA**]=10^6 molecules cm^{-3}. [**A**]=10^9 molecules cm^{-3}. T=220K.

[GA]	20%	40%	60%	80%	100%
10^7	1.03×10^2	1.04×10^2	1.06×10^2	1.07×10^2	1.09×10^2
10^8	1.10×10^2	1.12×10^2	1.14×10^2	1.17×10^2	1.21×10^2
10^9	1.91×10^2	1.96×10^2	2.11×10^2	2.45×10^2	2.76×10^2
10^{10}	2.43×10^3	2.58×10^3	3.15×10^3	4.53×10^3	5.97×10^3
10^{11}	1.69×10^5	1.83×10^5	2.30×10^5	3.37×10^5	4.39×10^5

Table S89. The formation rates (J, cm^{-3} s^{-1}) of $(\mathbf{GA/GW})_x \cdot (\mathbf{SA})_y \cdot \mathbf{A}_z$ clusters with the vabriations of the concentration of **SA** ([**SA**]) **and A** ([**A**]) at 220K. RH=50%. [**GA**]=10^9 molecules cm^{-3}.

| [SA] \ [A]	10^7	10^8	10^9	10^{10}	10^{11}
10^4	1.31×10^{-4}	2.50×10^{-4}	3.44×10^{-4}	1.80×10^{-3}	2.27×10^{-1}
10^5	1.29×10^{-1}	2.39×10^{-1}	3.27×10^{-1}	1.65	1.47×10^2
10^6	9.99×10^1	1.57×10^2	2.02×10^2	7.91×10^2	2.77×10^4
10^7	2.02×10^4	3.03×10^4	3.73×10^4	1.15×10^5	2.12×10^6

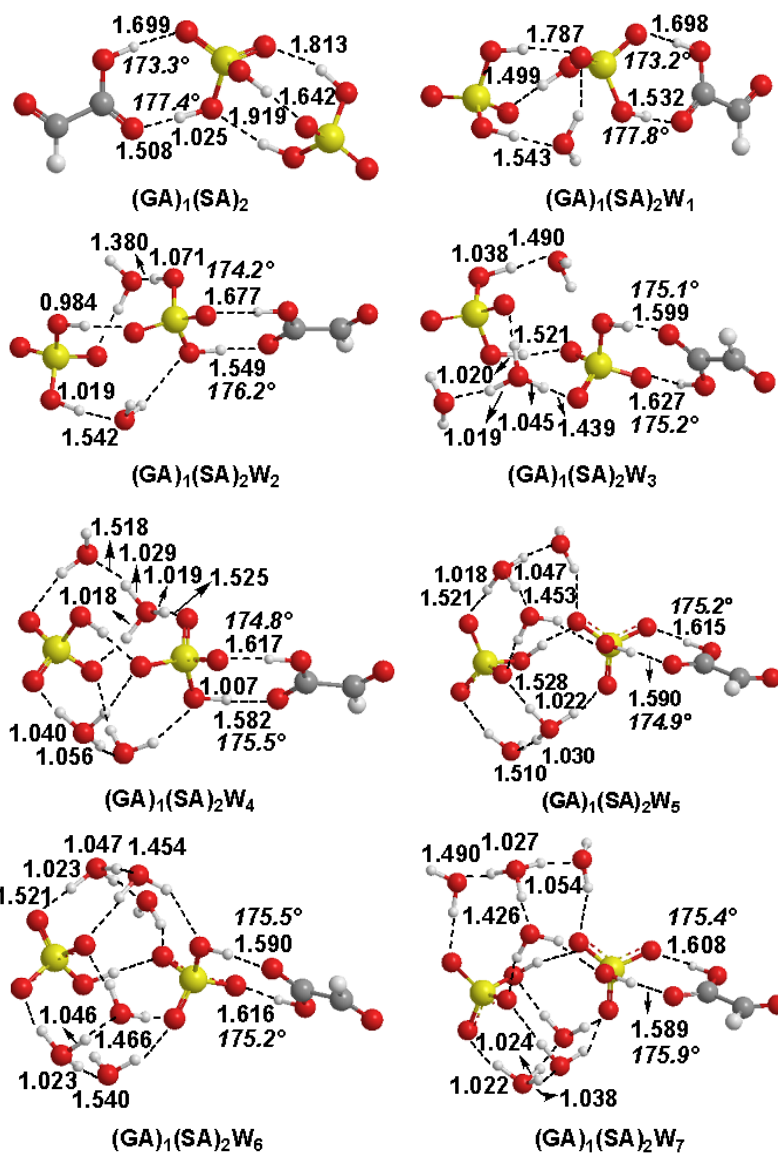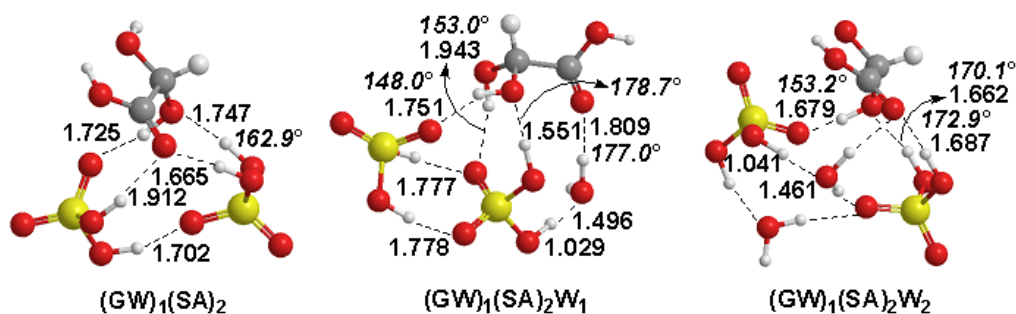|					
10^8	7.28×10^5	2.68×10^6	3.87×10^6	9.92×10^6	8.17×10^7
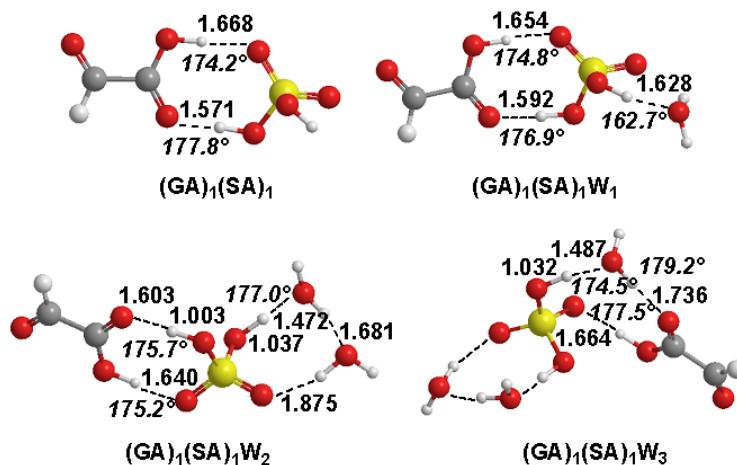
Figure S1. Most stable configuration of clusters $(GA)_1 \cdot (SA)_1 \cdot W_n$ (n=0-3). The lengths of the hydrogen bonds are given in Å. The hydrogen bonds are shown as dashed lines.
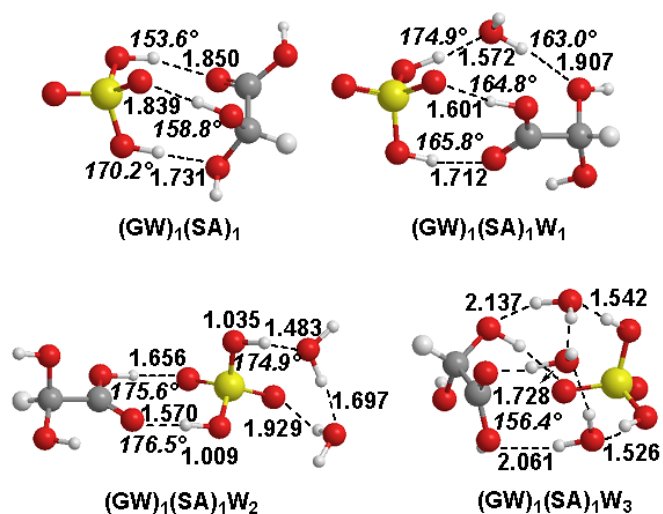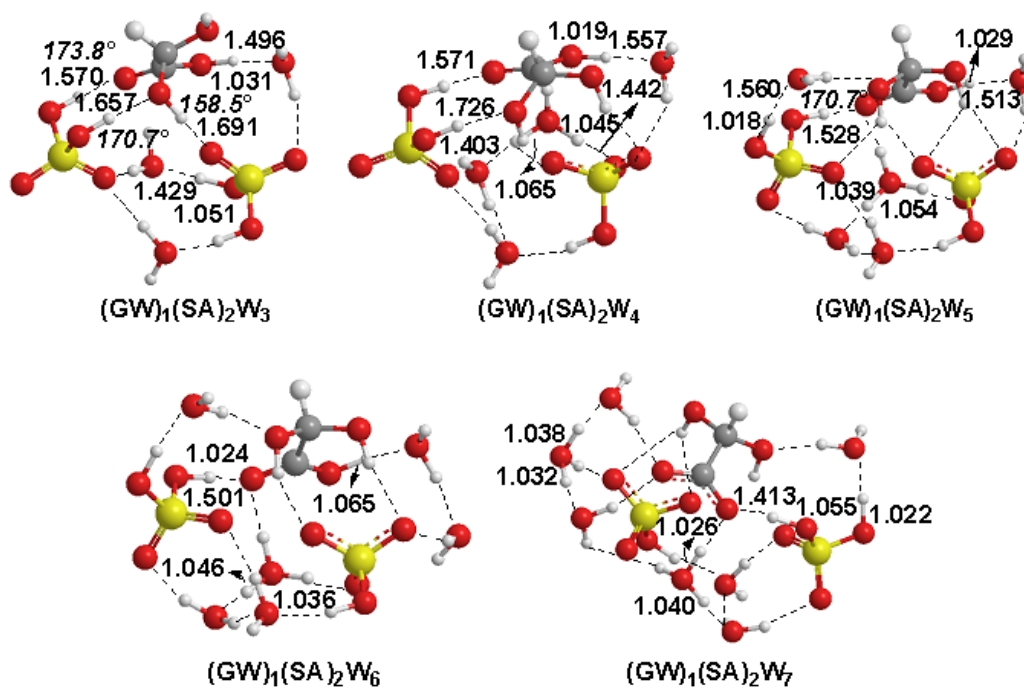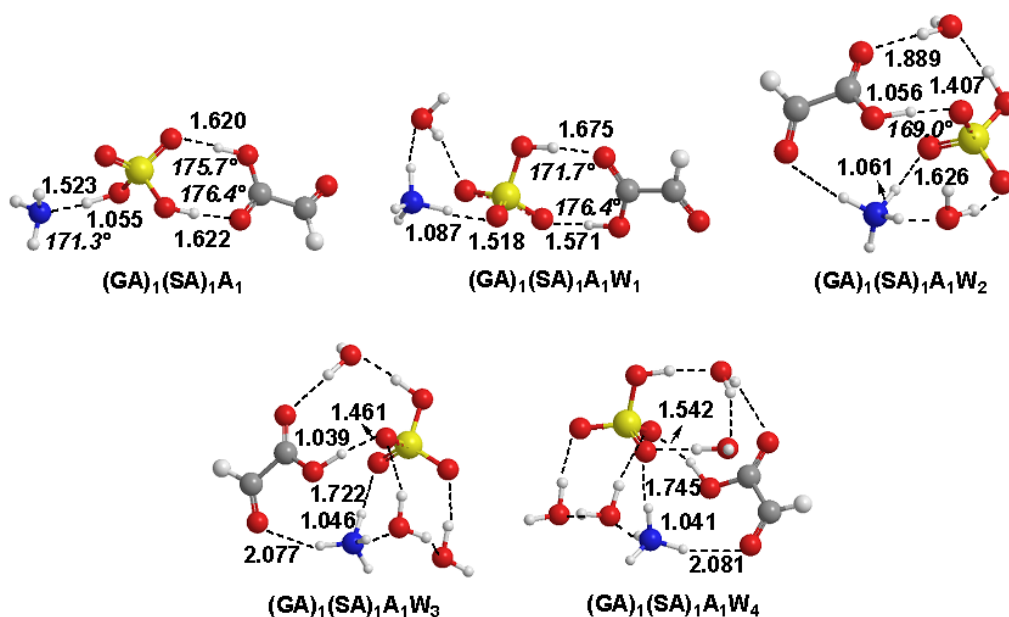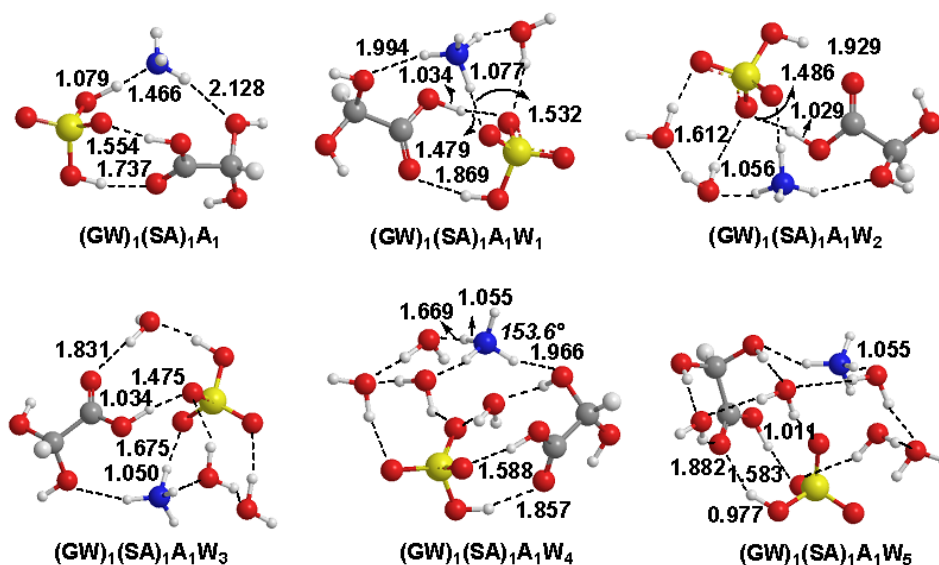

Figure S2. Most stable configuration of clusters $(GW)_1 \cdot (SA)_1 \cdot W_n$ (n=0-3). The lengths of the hydrogen bonds are given in Å. The hydrogen bonds are shown as dashed lines.

Figure S3. Most stable configuration of clusters **(GA)₁·(SA)₂·Wₙ** (n=0-6). The lengths of the hydrogen bonds are given in Å. The hydrogen bonds are shown as dashed lines.

Figure S4. Most stable configuration of clusters $(GW)_1 \cdot (SA)_2 \cdot W_n$ (n=0-7). The lengths of the hydrogen bonds are given in Å. The hydrogen bonds are shown as dashed lines.

Figure S5. Most stable configuration of clusters $(GA)_1 \cdot (SA)_1 \cdot A_1 \cdot W_n$ (n=0-4). The lengths of the hydrogen bonds are given in Å. The hydrogen bonds are shown as dashed lines.

Figure S6. Most stable configuration of clusters $(GW)_1 \cdot (SA)_1 \cdot A_1 \cdot W_n$ (n=0-5). The lengths of the hydrogen bonds are given in Å. The hydrogen bonds are shown as dashed lines.
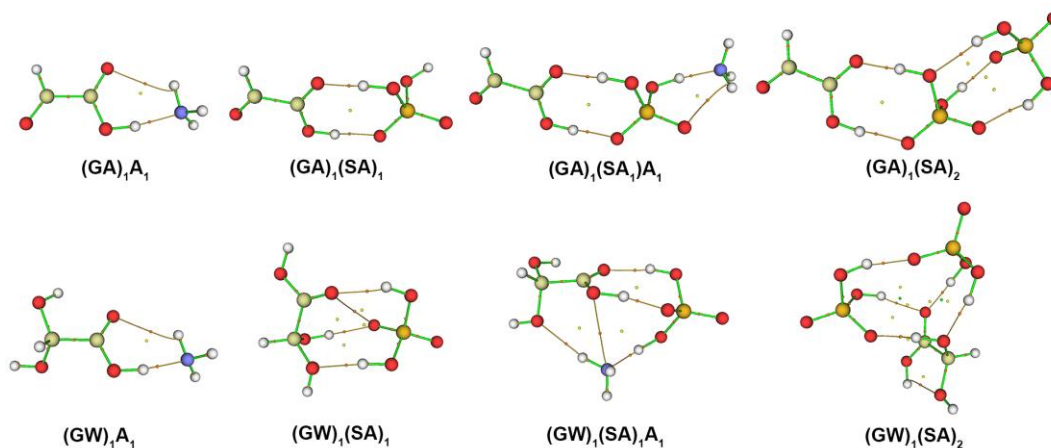
Figure S7. The AIM plots of the unhydrated clusters calculated at the M06-2X/6-311++g(3df,3pd) level. The bond critical points and ring critical points are presented by the ginger and yellow balls, respectively.
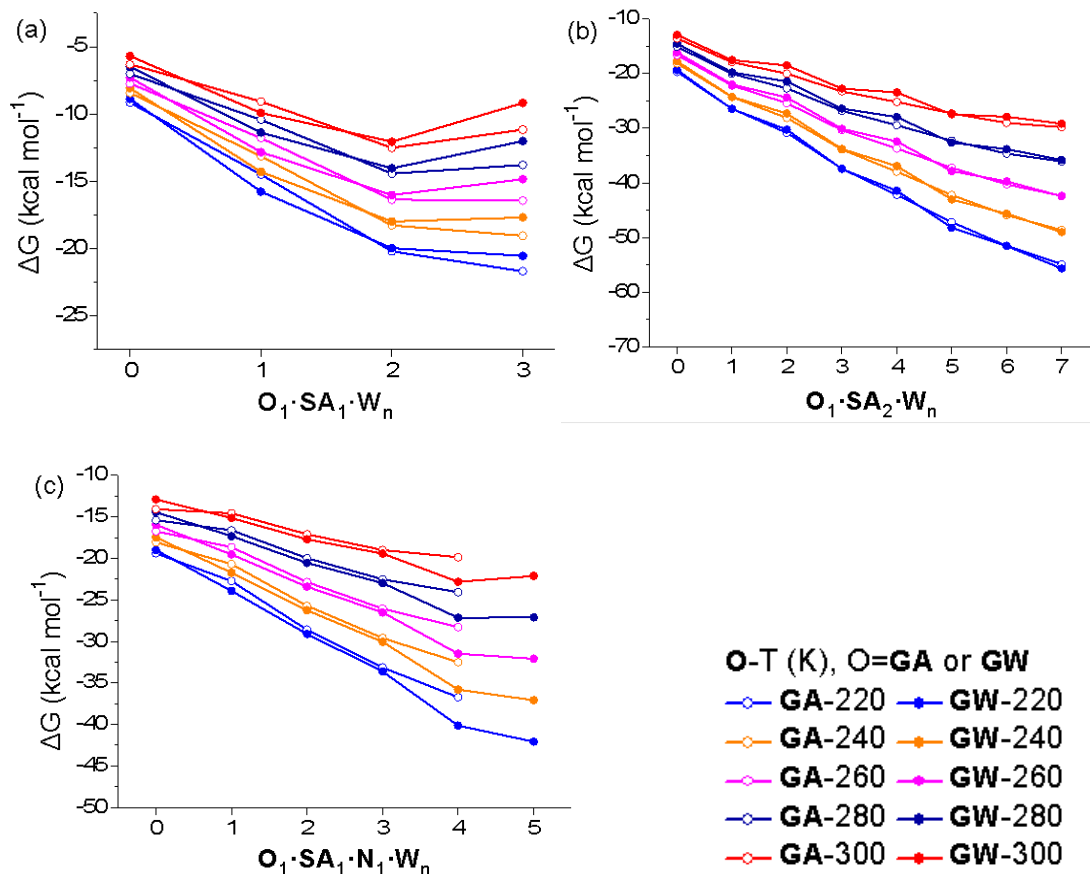
Figure S8. Gibbs free energies (kcal mol^{-1}) of formation of clusters (a) $O_1 \cdot SA_1 \cdot W_n$, (b) $O_1 \cdot SA_2 \cdot W_n$ and (c) $O_1 \cdot SA_1 \cdot N_1 \cdot W_n$. **O** indicates **GA** or **GW**.
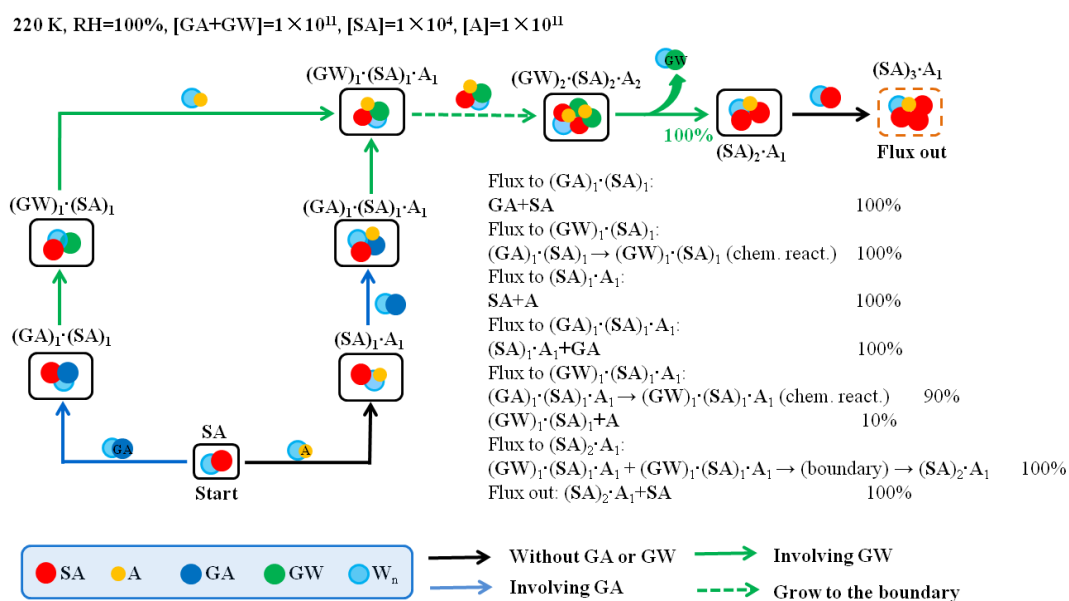
Figure S9. Main cluster formation pathways considering the hydration reaction of **GA**

forming **GW** are represented by arrows. Relative amounts of clusters formed via dominating growth pathways are indicated in the side table.

Section 2. Boundary Conditions

The boundary conditions require the outgrowing clusters to have a favorable composition so that the clusters leaving the studied size range are stable enough not to evaporate back immediately. The sum of all evaporation rate coefficients (Table S5) corresponding to different evaporating molecules from the clusters involving **GA** or **GW** are relatively high. The ammonia molecule also easily evaporates from cluster $(\mathbf{SA})_2 \cdot \mathbf{A}_2$.[2] Thus, clusters involving molecule **GA** or **GW** and cluster $(\mathbf{SA})_2 \cdot \mathbf{A}_2$ can not be considered stable enough to grow out of the studied cluster sizes. In contrast, the cluster $(\mathbf{SA})_3 \cdot \mathbf{A}_1$, with a maximum evaporation rate coefficient of 55 s^{-1} at 300 K, is relatively stable enough to resist evaporation. Thus, the boundary condition was set to be the cluster $(\mathbf{SA})_3 \cdot \mathbf{A}_1$. Using this relatively small cluster as a boundary condition might overestimate absolute NPF rates, but it is probably sufficient for probing the relative effect of **GA/GW** on cluster formation rate, which is the purpose of this study.

Complete Gaussian 09 reference (Reference 52)

Gaussian 09, Revision A.1,
Frisch, M.J., Trucks, G.W., Schlegel, H.B., Scuseria, G.E., Robb, M.A., Cheeseman, J.R., Scalmani, G., Barone, V., Mennucci, B., Petersson, G.A., Nakatsuji, H., Caricato, M., Li, X., Hratchian, H.P., Izmaylov, A.F., Bloino, J., Zheng, G., Sonnenberg, J.L., Hada, M., Ehara, M., Toyota, K., Fukuda, R., Hasegawa, J., Ishida, M., Nakajima, T., Honda, Y., Kitao, O., Nakai, H., Vreven, T., Montgomery, J.A., Peralta, J.E., Ogliaro, F., Bearpark, M., Heyd, J.J., Brothers, E.,

Kudin, K.N., Staroverov, V.N., Kobayashi, R., Normand, J., Raghavachari, K., Rendell, A., Burant, J.C., Iyengar, S.S., Tomasi, J., Cossi, M., Rega, N., Millam, J.M., Klene, M., Knox, J.E., Cross, J.B., Bakken, V., Adamo, C., Jaramillo, J., Gomperts, R., Stratmann, R.E., Yazyev, O., Austin, A.J., Cammi, R., Pomelli, C., Ochterski, J.W., Martin, R.L., Morokuma, K., Zakrzewski, V.G., Voth, G.A., Salvador, P., Dannenberg, J.J., Dapprich, S., Daniels, A.D., Farkas, O., Foresman, J.B., Ortiz, J.V., Cioslowski, J., Fox, D.J., 2009. Gaussian 09, Revision A.1, Gaussian Inc. Wallingford CT.

Reference

1 Ling Liu, Xiuhui Zhang, Zesheng Li, Yunhong Zhang and Maofa Ge. Gas-phase Hydration of Glyoxylic Acid: Kinetics and Atmospheric implications. Chemosphere. 2017, 186, 430-437.

2 I. K. Ortega, O. Kupiainen, T. Kurtén, T. Olenius, O. Wilkman, M. J. McGrath, V. Loukonen, and H. Vehkamäki. Atmos Chem Phys, 2012, 12, 225-235.